Letters in Applied NanoBioScience
Open-Access Journal (ISSN: 2284-6808)

Review
Volume 15, Issue 1, 2026, 37
https://doi.org/10.33263/LIANBS151.037

Synthesis Strategies and Emerging Applications of Carbon Quantum Dots – A Review

Swagatika Patnaik [1], Biswajit Dalai [2,3,*], Santoshi Labala [1], Kishanlal Meher [1], Nachiketa Mahala [1], Sarat Kumar Dash [4,*]

[1] PG Scholars, Department of Physics, School of Sciences, GIET University, Gunupur -765022, Odisha, India
[2] Department of Physics, School of Sciences, GIET University, Gunupur -765022, Odisha, India
[3] Department of Physics, School of Applied Science and Humanities, Haldia Institute of Technology (HIT), Haldia, Purba Medinipur - 721657, West Bengal, India
[4] Department of Physics, Regional Institute of Education, NCERT, Bhubaneswar – 751022, Odisha, India
* Correspondence: biswajit@giet.edu (B.D.); ddalai@hithaldia.ac.in, skdash59@yahoo.com

Received: 23.05.2024; Accepted: 1.11.2025; Published: 30.03.2026

Abstract: In this review work, we have highlighted the synthesis techniques, characteristics, and applications of carbon quantum dots (CQDs / CDs). This CQD is a noble class of nanomaterials containing carbon with zero dimension. CQDs have a particle size between 1 and 10 nm. Because of the characteristics of CQDs, i.e., intense fluorescence, tiny size, superconductivity, and rapid electron transfer, their composites have high electric conductivity and catalytic activity. Furthermore, the abundant surface functionalities on CQDs may enable the formation of multi-component electrically active catalysts. This multicomponent catalyst's interaction may facilitate charge transfer, an essential electrochemical process. The different properties of CQDs are largely dependent on the synthesis methods used. A variety of synthesis methods, including hydrothermal techniques, microwave synthesis, arc discharge, and pyrolysis, were used to synthesize CQD. Its intriguing qualities make it a mystic luminary in nanoscience. The importance of CQDs stems from their diverse applications, driven by their unique optical, electronic, biocompatibility, and physicochemical properties. Other benefits of CQDs include their non-toxicity, high efficiency, environmental friendliness, high chemical stability, exceptional water solubility, and low production cost, which have drawn the attention of researchers to CQDs for commercial applications.

Keywords: carbon quantum dots (CQDs/CDs); synthesis; characteristics; applications.

1. Introduction

With around 8 billion people on the planet, various industries produce enormous amounts of waste, and to fulfill the sustainability concept, scientists are working on valuable resources [1-4]. To extract single-walled carbon nanotubes from a mixture of weakly fluorescent carbon nanomaterials, a method called gel electrophoresis was developed. Nanoscale carbon particles are produced by laser ablation of a carbon target [4]. The Lycurgus cup, discovered in the ancient Roman period, is composed of solid lime, gold, and silver nanoparticles, created by a Roman glassmaker. Fundamentally, carbon-based intensifiers called carbon quantum dots (CQDs) are additionally referred to as nanoparticles, with sizes approximately 10 nm. Because of their distinctive qualities—such as their tiny size,

biocompatibility, high temperature stability, chemically inert structure, ease of functionalization, and non-toxicity- CQDs are typically used in a wide variety of fields [5-7]. Since CQDs are synthesized through numerous chemical treatments, they have a strong ability to bind both organic and inorganic molecules. Chemiluminescence and electrochemical luminescence are caused by the remarkable electrical property [8, 9]. CQDs are generally defined as spherical nanoparticles that are monodisperse and consist of a carbonaceous core with a few useful groups attached to its surface. It has demonstrated efficacy in a variety of sophisticated biological applications, including as a filler for composite manufacturing, an environmental remediation sensor, and a catalyst.

Carbon dots refer to a rather diverse group of nanoparticles with varying chemical and optical characteristics. The fluorescence emergence mechanism is detachable, and in certain cases, particularly with citric acid, the fluorescence is caused by molecular and molecular-like states [10-12]. In addition to standard or down-converted photo luminescent, which enables sophisticated photodynamic therapy with excellent performance, near-infrared (NIR) photoluminescence (PL) is a possible feature of C-Dots. Their applications are further expanded by the spectral region under NIR light excitation [11, 12]. Due to the remarkable photo stability and fluorescence characteristics of CQDs, they have potential applications in various fields, including biomedicine, catalysis, and optoelectronics, and have a green synthesis process. In this work, the materials and methods, characterization processes, various optical properties, and emerging biomedical and optoelectronic applications of CQDs were discussed.

2. Materials and Methods

Various enormous scope, effectively versatile, and sensibly valued production techniques have been developed after the disclosure of CQDs. Two broad categories were used for the synthesis of CQDs, i.e., top-down and bottom-up methods (Figure 1).

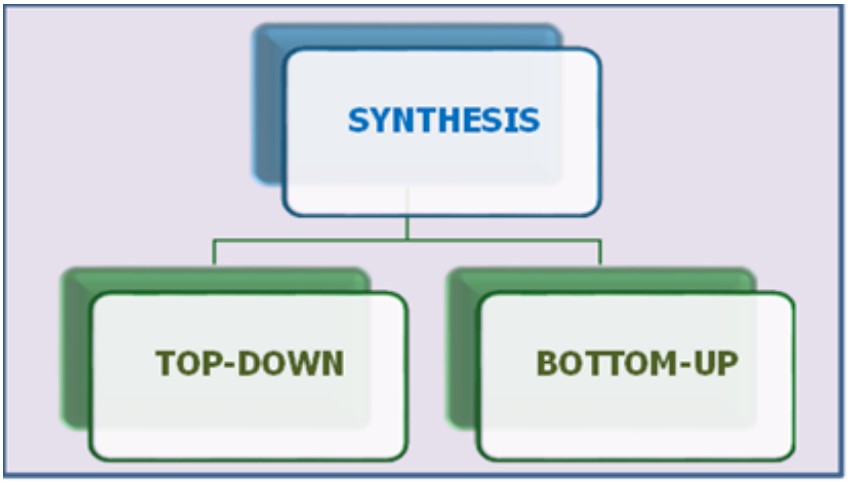

Figure 1. Synthesis methods for CQDs.

The synthesis of CQDs is simple, whereas certain difficulties are involved [10-12]. CQDs doped with metals like Au or Mg or heteroatoms like N and P, boost electrical conductivity and solubility [12, 13]. Both methods (Figure 2) have been used for the synthesis of CQDs, but the bottom-up approach is more commonly used because it is more economical and environmentally friendly [13, 14].

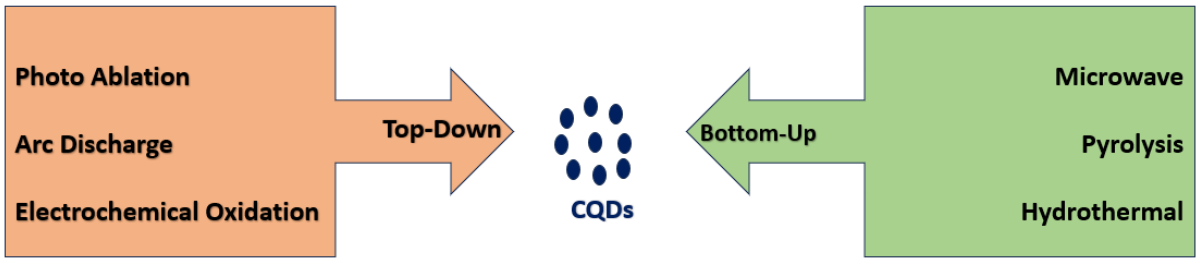

Figure 2. Various types of synthesis routes under the top-down and bottom-up methods.

2.1. Top-down route.

Top-down and bottom-up synthesis form an intricate structure (Figure 3). Using a variety of techniques, the precursor's bulk structure is broken down into materials with nanostructures. Carbon's intricate structures, such as graphite, nanodiamond, carbon soot, and carbon nanotube, are transformed into quantum dots. Large carbonaceous materials can be reduced to nanostructures by means of photoablation, arc discharge, and acidic oxidation [14, 15].

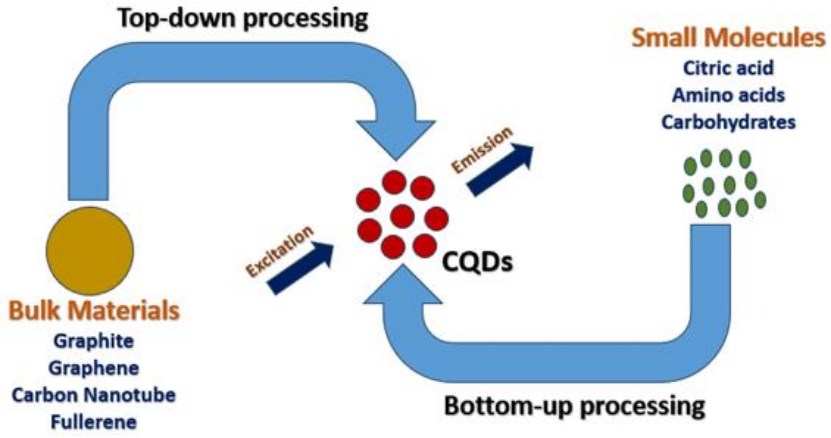

Figure 3. Schematic diagram of top-down and bottom-up processes.

2.1.1. Photo ablation.

Photoablation is one technique that uses light energy to ablate a carbon target [16-23]. The carbon target was initially developed by Sun *et al*. [16] with the assistance of warming a graphite and cement blend. The target carbon was further removed using a focused light beam at 900°C and 75 kPa in an argon gas flow containing water vapour to produce carbon nanoparticles. They were able to create bright C-dots with this approach. The prepared nanoscale carbon particles were detected as an accumulation of varying sizes and showed no observable photoluminescence (PL). The material was lastly treated with polyethylene glycol or polypropionylethyleneimine-coethyleneimine, following a 12-hour reflux in a dripped nitric acid solution. The resulting C-dots were extremely photoluminescent, passivated, and were around 5 nm in size. Direct laser ablation was used to produce carbon nanoparticles from carbon targets by dissolving the targets in deionized water; the resulting particles were non-fluorescent. The zero-dimensional carbon was disintegrated in a nitric acid solution and refluxed for 12 hours to activate its surface. After that, the carbon nanoparticles were refluxed for an additional 28 hours in a PEG200 solution. After adding mecaptosuccinic acid, the carbon nanoparticles were refluxed for a further thirty-one hours. Finally, colourless to light brown fluorescent C-dots with an average diameter of 267 nm were formed from the solution. The

complex life-span degradation of the C-dots with functionality was unaffected by the length of the PEG chain or the presence of additional modifiers. It is possible to detect iodide using C-dots because iodide can quench their fluorescence. Other metal ions such as Hg(II), Cu(II), Cd(II), Ni(II), Zn(II), and Ca(II) did not show any noticeable impact on the C-dots' fluorescence. Uncover graphite chips found by Hu *et al* [20] by utilizing a pulsed laser for radiation. Usually 2 μm in size, added to the PEG1500N solution, and ultrasound was utilized for four hours throughout the laser exposure process, resulting in a consistent black suspension. C-dots were isolated from the bright Supernatant via sedimentation at 5000 rpm. The pulse timing of the millisecond-pulsed laser, the C-dots, ributions, and topographical features can be checked and then assessed despite many advantages, such as their intuitiveness and the ability to create a diverse range of nanoscale objects, larger carbon nanoparticles are easily removed during centrifugation, resulting in low yields and low carbon utilization efficiency. There is a significant variation in the diameters of the carbon nanoparticles, produced by laser irradiation.

2.1.2. Arc discharge.

According to Arora and Sharma [24], this process entails rearranging carbon molecules as they break down, utilizing gaseous plasma, created in a fixed reactor, using mass carbon sources. The reactor may reach 3727℃ under the electric current, producing extremely energetic plasma. In the positive terminal, carbon vapour condenses to produce CQDs. It may display different colour fluorescence at 365 nm. The carboxyl group (-COOH) was applied to the surface using HNO_3 on CQDs. The CQDs produced by this method often have excellent water solubility, are 18 nm in size, and can be of unequal sizes. A comparatively poor yield of carbon atoms is formed during the arc-discharge procedure. Moreover, it may be difficult to filter and eliminate some of the complex components found in nanoparticles produced by arc discharge. Chao-Mujica *et al*. [26] utilized a new strategy to make CQDs in water. The generated CQDs showed a 16% quantum yield and two consistent bands, A and B, of range $2.75 \times 10{-}7\ m$ and $2.85 \times 10{-}7\ m$, respectively. As the excitation wavelengths range from 320–340 nm and 400–410 nm, these CQDs were used as a fluorophore in in vitro experiments on L929 murine fibroblasts in cell culture. CQDs may be used for bio-imaging applications. Limited particle size and low QY scalability were observed in this type of CQD [24-27]. It had not demonstrated a strong PL feature.

2.1.3. Electrochemical oxidation ~~[26-30]~~.

To cause the anode to react with oxygen and serve as the carbon source from the carbon nanoparticles, this strategy usually entails applying a specific voltage or current to the carbon working cathode, which has conductive properties [26-30]. After centrifugation, carbon dots are obtained. Li *et al*. [29] employed pure water as the only electrolyte to create CQDs by electrochemically oxidizing graphite rods. Polymers are passivated and carbonized further to produce CQDs. During the solution's electrolysis, the cathode and anode produced NaCl, H_2, and Cl_2, and these elements are important for the synthesis of CQDs. Ran *et al*. [30] work on CQDs incorporates one more process, utilizing a one-pot electrochemical methodology. They used a three-electrode setup to create CQDs by utilizing alcohol. As the working and counter electrodes, two sheets of platinum (Pt) were used. Here, calomel electrodes served as the reference electrode that was attached to a lugging capillary. Rubber plugs were allowed to adjust the distance of the electrode. Alcohol is electrochemically carbonized into minuscule

particles that offer a quick method for making quality CQDs. This technology has the following benefits: it is inexpensive, simple to use, allows the manufacture of CQDs with tunable emission wavelengths under various synthesis conditions, and offers ample opportunity to prepare both long-wavelength and multicolor short-wavelength emissions.

2.2. Bottom-up route.

Bottom-up synthesis (Figure 3) is a method used to create CQDs from chemical precursors. With this method, CQDs are produced chemically by reacting small molecules. The hydrothermal process, microwave synthesis, and pyrolysis are various routes of the bottom-up methodology [22, 26, 30, 31]. The hydrothermal method involves dissolving the precursor molecules in water and storing them in a stainless steel autoclave coated with Teflon. Then the autoclave is placed inside the hydrothermal chamber for a few hours at a high temperature and pressure. Proteins, polymers, glucose, amino acids, citric acids, carbohydrates, and certain waste products and naturally occurring substances are utilized in synthesis and are examples of precursor molecules. The hydrothermal process is a one-step, nontoxic, affordable, and environmentally friendly procedure. It has attracted a lot of attention in current research [32-38]. A range of beneficial properties, including high homogeneity, water solubility, monodispersity, photo stability, salt tolerance, controlled particle size, and improved QY without surface passivation, is achieved through hydrothermal treatment of CQDs. It yields CQDs via solvothermal synthesis, a process similar to hydrothermal synthesis [39-41].

2.2.1. Microwave synthesis.

Synthesis using microwave routes in carbonizing small organic molecules is achieved by heating them with a microwave [42-51]. Zhu *et al*. [41] employed a microwave technique to vary the microwave processing time to produce amorphous products with varying sizes and luminosities. Liu *et al*. [42] created luminous CDs by microwave heating glycerol as the carbon source and 4,7,10-trioxo-1,13-tridecylenediamine as a surface passivation specialist. The PL quantum yield was 12%, and the particle size was 5-7 nm. Despite the low yield of CDs, it was found that by adding N atoms to them, their fluorescence properties were increased [42, 43]. Liu *et al*. [42] increased the PL quantum yield to 15–20% by using branching PEI (~ 25 kDa) as the role of corrosion inhibitor and to create amino-rich CDs. Since the carbon precursors can be heated more quickly and easily than with earlier techniques, i.e., the synthesis process is more streamlined. Hence, CDs may be readily and rapidly obtained, and their production can be increased. These noble, environmentally friendly, and efficient techniques can be used to synthesize nanomaterials. Due to the irregular particle size distribution, separation and purification are quite difficult.

2.2.2. Pyrolysis.

In certain applications and mechanistic investigations, to achieve homogeneous features through CQD diameter control is imperative. To obtain stable CQDs, fragments were purified by filtration, dialysis, centrifugation, column chromatography, and gel electrophoresis [52-55]. It is possible to create discrete CQDs with standardized, adjustable sizes via meticulously controlled pyrolysis of a naturally occurring precursor in nanoreactors. Three processes were employed: (i) using thin power, the natural precursor was incorporated into permeable nanoreactors; (ii) the natural precursor was pyrolyzed within the nanoreactors to

supply carbonaceous matter; and (iii) the synthetic CQDs were then supplied. Absorbent silica nanoreactors are the most commonly used due to their ease of removal, thermal stability, and a variety of easily tunable textures. Zhu *et al*. [41] produced hydrophilic CQDs that may be utilized as nanoreactors by impregnating mesoporous silicon nanospheres with a precursor of citric acid.

2.2.3. Hydrothermal.

Hydrothermal (HT) processes for preparing CQDs and their derivatives have attracted significant interest due to their advantages of cleanliness, cost-effectiveness, and efficiency [56-59]. HT processes provide an efficient method for preparing CQDs and their derivatives via hydrolysis, polymerization, and carbonization reactions. HT processes provide a green route to produce carbon-based nanomaterials from various precursors, including chemical compounds, biomass, and other carbon sources. HT-CQDs are fabricated in subcritical liquid water, involving a carbonization process to convert carbon precursors into CQDs at a moderate temperature (180–250°C) and self-built pressures (2–6 MPa) [28,29], as illustrated in CQD synthesis by HT consists of four steps: hydrolysis, polymerization, carbonization, and passivation (Figure 4).

Figure 4. Various steps of the hydrothermal (HT) processes to prepare CQDs.

Initially, large organic molecules are hydrolyzed into smaller molecular fragments in an aqueous environment, where high temperature and pressure break down chemical bonds. These fragments then undergo dehydration, losing water molecules and becoming more reactive, followed by polymerization, during which they combine to form the complex, large polymeric structure. The resulting polymers are subjected to carbonization, which transforms them into condensed carbon clusters composed of sp2-hybridized carbon atoms. As the reaction advances, these clusters nucleate and coalesce into the discrete, nanoscopic crystalline structures known as CQDs. CQDs have been obtained by hydrothermal synthesis with average sizes ranging from 4 to 15 nm.

3. Characterizations of CQDs

Carbon quantum dots can be characterised using a range of methods, including transmission electron microscopy (TEM), X-ray diffraction (XRD), Fourier transform infrared spectroscopy (FTIR), field emission scanning electron microscope (FESEM), nuclear magnetic resonance (NMR), and UV spectroscopy [60-70].

3.1. Transmission electron microscopy (TEM) ~~[69-72]~~.

Because of its high resolution of 0.1-0.2 nm, transmission electron microscopy (TEM/HRTEM) is widely used across the fields of science, pharmaceuticals, materials science, and other research domains [69-72]. It is also used to investigate the morphology of nanoparticles to learn more about their size, shape, and dispersion. The analysis of carbon dots (C-dots) is commonly done using TEM. Moreover, the precise configuration of carbon dots can be determined using high-resolution transmission electron microscopy. There are two forms of lattice fringe: interlayer spacing and in-plane lattice spacing, which are crystalline in nature and may be differentiated from each other. While interlayer spacing is usually

concentrated at about 0.34 nm, and in-plane lattice spacing is often sought at 0.24 nm. When graphite was acid-oxidised by Zhang et al. [69], the resulting carbon dots exhibited a lattice spacing of less than 0.3 nm. That suggests a sizable portion of the dots were, in fact, unique graphenes. At the point when Shinde *et al*. [70] orchestrated C-dots from MWCNT, various kinds of grid edges were found in the HRTEM by using an electrochemical method.

3.2. X-Ray diffraction method (XRD).

It is a method for characterising carbon dots and learning important details about their phase purity, crystal structure, and particle size. It is also necessary to ascertain the crystalline phases of CQD [73-77]. Hexa-perihexabenzocoronene was the precursor employed by Liu *et al*. [74] to make the carbon dots. Ablation, adsorption, deoxidation, and chemical etching were used to make carbon dots. Their width was about 60 nm, and their thickness was about 2-3 nm. The resulting carbon dots showed a quantum yield of fluorescence of 3.8%. Mao *et al*. [75] produced glowing C-dots by pyrolyzing poly(acrylic acid) in one stage using glycerol. The optical and structural properties of the carbon dots were examined. The white fluorescent carbon dots graphite structure is further supported by the broad peak around $2\theta = 24°$. The matching X-ray diffraction pattern showed two superimposed reflections when carbon dots were synthesised by Bourlinos *et al*. [72] by calcining ammonium citrate at 300°C, indicating the presence of an extraordinarily long alkyl carbon chain.

3.3. Fourier transform infrared spectroscopy (FTIR).

The surface-associated groups of carbon dots have also been identified through the use of Fourier transform infrared spectroscopy (FTIR). Hydrogen, carbon, and oxygen are the three primary ingredients of carbon dots [78-80]. The surface of carbon dots contains many carboxylic acid, hydroxyl, and ether/epoxy groups because they are made by partially oxidising carbon precursors. FTIR is a helpful technique for analysing these oxygen-containing compounds. It is possible to characterise modified C-dots and assess whether they are sufficiently passivated using infrared spectroscopy. Peng *et al*. [77] produced 1-4 nm carbon dots from chemically oxidising micron-sized carbon strands. Dimethyl sulfoxide and dimethyl formamide were used to show particle decomposition in a polar solvent and in water. The existence of a carboxyl group was suggested by the typical absorption peaks at 1724 cm^{-1} and 3307 cm^{-1}. The presence of a double bond was suggested by the absorption peak at 1579 cm^{-1}, and the presence of an ether linkage was suggested by the absorption peak at 1097cm^{-1}.

3.4. Field emission scanning electron microscope (FESEM) ~~[81, 82]~~.

The different structures and properties of the prepared CQDs were studied with the help of FESEM [81, 82]. Nitrogen-doped carbon quantum dots (NCQDs) were synthesized from the tropical plant Litsea glutinosa using an environmentally friendly, time-efficient hydrothermal method. NCQDs exhibited strong and stable green fluorescence. Ugi reaction was utilized to modify the surface of CQDs, an environmentally friendly hydrogen-bonding nanocatalyst. The CQDs were produced via a hydrothermal method using citric acid and urea, and then coated onto magnetic Fe_3O_4 nanoparticles. Comprehensive characterization using FTIR, FESEM-EDX, XRD, XPS, zeta potential, Raman, and HRTEM confirmed the optical, structural, and morphological properties of the CQDs.

3.5. Nuclear magnetic resonance (NMR) ~~[79, 81-83]~~.

The structure of carbon dots is commonly studied using the nuclear magnetic resonance (NMR) technique [81-83]. ^{13}C-NMR is used to determine the mechanism between carbon atoms and hybrid forms of C-atoms in the crystalline network. Tian *et al*. [78] had utilised natural gas sediment consuming as a source of carbon, followed by nitric acid refluxing to create carbon dots. Carbon dot structural features are ascertained using NMR. Though aliphatic (sp3) carbons show reverberation in the scope of 8-80 ppm, aromatic (sp2) carbons show reverberation in the scope of 90-180 ppm. Under the non-aromatic carbon group, there was no single top, as the 13C NMR range showed 120 ppm. Between 120 and 150 ppm, a spectrum of peaks developed, the bulk of which were caused by aromatic carbons. The carbon dots were made of sp2 carbons.

3.6. UV spectroscopy.

Strong ultraviolet (UV) absorption is a characteristic of carbon dots produced by a range of processes [82-85]. However, the positions of the UV absorption peaks differ significantly depending on the technique used to prepare the C-dots. The near infrared (NIR) (800 – 2400 nm), visible (400-700 nm), and UV (200-400 nm) zones of transmission were represented by the sizes of C-dots, which are 3.8, 1.5-3, and 1.2 nm, respectively. Li *et al*. [79] sonicated a suspension for two hours at room temperature after mixing 4 g of active carbon with 70mL of hydrogen peroxide. Fluorescent water-soluble C-dots with a diameter of 5–10 nm were obtained after filtering. An aromatic pi structure was absorbed, as seen by the distinctive UV–visible density peak at 2.5 × 10−7 m to 3 × 10−7 m by Wang *et al*. [85]. After adding 0.5 g of anhydrous citrus extract, a solution of N-(β-aminoethyl)-γ-aminopropyl methyl dimethoxysilane (AEAPMS) was vigorously swirled for a minute at 240°C. Amorphous carbon was mixed with natural carbon nanoparticles, which had a diameter of about 0.9 nm. They also displayed a high brightness (quantum yield: 47%) upon cooling and purification. At 360 nm, the produced C-dots showed a notable peak of UV-visible absorption.

Citrus acid carbonation was utilized to create photo-luminescent C-dots at 200°C, and consequently, carbon dots were produced. Nanosheets with a thickness of 0.5-2.0 nm and a width of about 15 nm exhibited UV absorption, with a maximum at 362 nm. The maximal emission of wavelength was maintained when triggered at various excitation wavelengths. In order to manufacture C-dots, Tang *et al*. [84] performed pyrolysis of a glucose solution with the aid of a microwave. The resulting C-dots had a diameter of 1.65 nm and a fluorescence quantum yield of 7–10%. The aqueous solution of these C-dots revealed two separate peaks of UV absorption at 228 and 282 nm. In contrast, the peak of one of the UV absorption bands became more intense as the microwave heating time was extended.

4. Results and Discussion: Optical Properties of CQDs

CQDs are quasi-spherical carbon-based nanomaterials with small size, low toxicity, high quantum yield, good biocompatibility, eco-friendliness, high chemical stability, the ability to accelerate charge separation, improved electron mobility, increased photocatalytic activity, strong absorption, high water solubility, and unique optical properties (Figure 5).

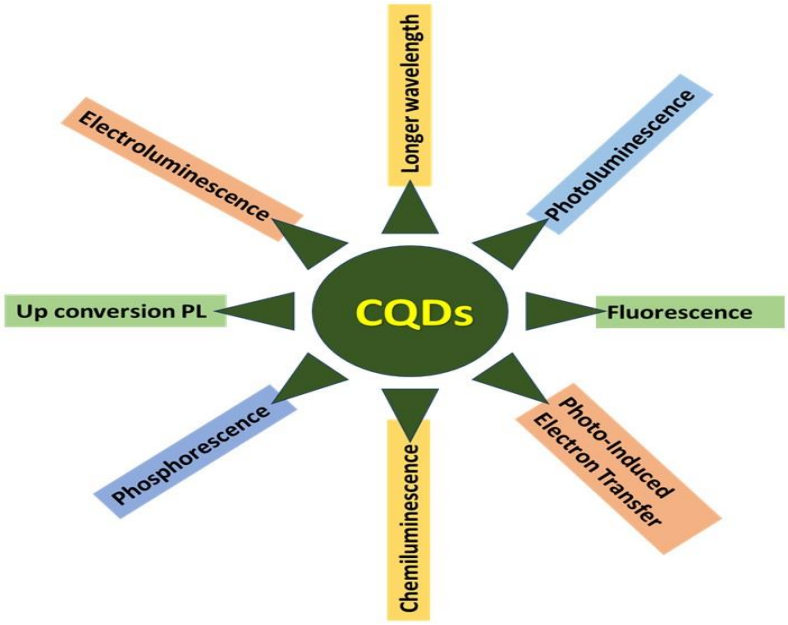

Figure 5. Various optical properties of CQDs.

They exhibit their primary optical absorption in the UV region (wavelengths between 250 and 320 nm), with a tail extending into the visible spectrum [85-98]. The positions of the UV absorption peaks on CDs made using various techniques differ significantly. The altered CDs will exhibit a rise in absorption wavelength. There might not be any discernible absorption peak at all. These absorption bands vary in position depending on the synthesis method and the raw precursors. The optical characteristics of CQDs can be changed by doping with spiropyrans, thiols, and other covering materials, i.e., a protective layer that acts as an insulator during the surface passivation process [99-111]. Thionyl chloride, oligomers of polyethylene glycol (PEG), etc., were formed on the surface of CQDs. These protective coatings are essential for stabilising CQDs and keeping impurities away from adhering to them. There may be metal doping, non-metal doping, and co-doping. Doped CQDs can alter their physicochemical properties and exhibit enhanced optical properties, improved charge-transfer efficiency, greater electron mobility, and increased photocatalytic activity [61, 62]. CQDs turn out to be highly optically dynamic and exhibit significant fluorescence, approaching an IR spectrum, when surface-passivating compounds are applied. Surface enhancement provides an alternative approach to boosting the quantum yields (QYs) of CQDs by 55–60%. The CQD absorbance was surface-enhanced using 4,7,10-trioxa-1,13-tridecanediamine (TTDDA) to reach longer wavelengths (350–550 nm). Zhu *et al*. [112] synthesised F-doped CQDs with enhanced QYs, electron transport, and photocatalytic activity through the use of a hydrothermal method.

4.1. Photoluminescence (PL).

CDs have good tunable PL behaviors [113-116]. The wavelengths of excitation (λex) determine the appearance and intensity of photoluminescent peaks (λem). As a result, getting several PL spectra from a single one is simple. The PL maximum for CDs typically appears in the blue and green parts of the spectrum. To control the PL behaviour of CDs, surface engineering, synthetic techniques, and early precursors can be applied. PL generated from CDs almost never changes over long periods of exposure to radiation, unlike organic dyes, which are photo-bleached. Sun *et al*. [114] reported a CD with a typical molecule size of around 1.54 nm. When stimulated at wavelengths of order 0.036 nm, 0.046 nm, and 0.054 nm, the

synthesized CDs show top maxima focused at roughly 0.046 nm, 0.054 nm, and 0.062 nm in their PL ranges. Wang *et al*. [115] revealed the production of N-CDs with exceptionally intense PL maxima from m-amino benzoic acid, with a peak observed at 415 nm. Additionally, they discussed the application of amine-passivated CDs as biosensors for pH and Fe3+ detection. Sun *et al*. [114] provided details about CDs that were passivated using PEG1500N, an oligomeric ethylene glycol. When the PL of these passivated CDs is quenched in the presence of N, N-diethyl aniline (DEA), Ag+, 2,4-dinitrotoluene, and 4-nitrotoluene, photo-induced electron transfer (PET) processes were seen in these CDs.

Even though a lot of research has been done on the physicochemical properties of CQDs, it is still unclear where the observed optoelectronic behavior came from. Photoluminescence characteristic of CQDs is not caused by a single condition but rather by a combination of factors connected to their particular properties. The process for creating CQDs by pyrolyzing precursors of ethanolamine (EA) and citric acid (CA) was verified at various temperatures. By dehydrating EA-CA, pyrolysis at 180°C produces a CQD precursor with a strong PL with high QY. A carbonaceous core forms at temperatures greater than 230°C. At this stage, the PL is influenced by both the carbonaceous core and the molecular fluorophores. CQDs with PL, exclusively derived from carbonaceous cores, were generated at temperatures of 300 and 400°C. The conditions under which CQDs are synthesized have a substantial impact on their PL behaviour.

4.2. Fluorescence.

Nano-scale materials, such as CQDs, have attracted significant attention over the last 10 years [117-133]. Even though the precise source of the particles' fluorescence emission is still unknown. Hence, more study is required to get a clear picture of the mechanism behind the emission of CQDs. Two widely accepted theories have been put forth to explain the particles' fluorescence mechanism: the conjugated p-domain bandgap emission and surface defect states. Again, two common mechanisms have been reported to provide a comprehensive explanation of CQD fluorescence. First, the fluorescence arises from a band-gap shift in the π-conjugated domains (sp2-hybridized); this is comparable to how aromatic compounds exploit specific energy band gaps to promote emissions and absorptions. The second explanation of fluorescence is related to surface defects, surface passivation/functionalization, surface flaws, and the carbon center state. The main sources of surface defects in CQDs are heteroatoms such as B, N, P, and S, as well as an unequal distribution of sp^2- and sp^3-hybridized carbon atoms. This surface imperfection forms environments resembling aromatic molecules when it integrates into the solid host. These compounds have the capacity to attract UV light and emit various hues. CQDs show two types of emission: excitation-dependent emission and excitation-independent emission. Because of their surface's various emission sites and particle size dispersion, the majority of CQDs show adjustable emissions. The highly organised graphitic structure of CQDs is responsible for their excitation and independent of emission. Continuous fluorescence and a wide, uninterrupted excitation spectrum are displayed by CQDs. Dual-emissive nitrogen-doped carbon dots (N-CDs) with yellow fluorescence were prepared by a one-step solvothermal method with o-phenylenediamine (OPD) and quercetin (QR) as precursors [133].

4.3. Upconversion PL.

Up-conversion fluorescence could result from the absorption of two photons [132-134]. Few CQDs are visible, with conversion photoluminescence (PL), even when excited at longer wavelengths. The peak maxima in discharge spectra appear at lower frequencies during upconversion of PL by irradiation at λex> 500 nm. CDs display evidence of upconversion and were used for He-La cell imaging. When the emission wavelength is shorter than the excitation wavelength, then up-conversion fluorescence happens. Here, the background auto fluorescence was reduced by longer excitation wavelengths and distinct labeling with a variety of emission wavelengths, i.e., up-conversion fluorescence. CDs treated with ultrasonic radiation exhibit wavelength-shifted fluorescence. After activation at 650–1,000 nm, CDs based on glucose and ammonium hydroxide exhibited up-conversion emission in the 300–600 nm range.

4.4. Longer wavelength.

When CDs were subjected to UV light, they emitted blue fluorescence, and biological analysis uses blue-emitting CDs, which are readily detectable because blue fluorescence is emitted by biological tissues and cells [115, 131-134]. Longer-wavelength CDs were prepared using a variety of techniques, including surface modification, size control, and pH regulation. The presence of heteroatoms such as nitrogen and oxygen led to a red shift in the discharge frequency, despite the blue-to-green/yellow fluorescence. The development of a large conjugated π system has simplified the production of red fluorescent CDs. CDs with longer emission wavelengths exhibited a fluorescence mechanism. Yuan *et al*. [117] developed extremely luminous CDs from blue to red by extending the conjugated π system. This would protect tissues from potential harm and lessen the spectral interference from fluorescent signals. Using p-phenylenediamine, 1,3-dihydroxynaphthalene, and the three-fold symmetric phloroglucinol as a precursor, the red-fluorescent CDs with high QY can be made.

4.5. Phosphorescence.

CDs have possibilities for displays and illumination [134-137]. Its polyvinyl alcohol (PVA) matrix showed phosphorescence, and its fluorescence was also noticed. The long duration of about 380 ms of phosphorescence was ascribed to C=O bonds on its surface. On the basis of a CD–PVA composite film, they have acquired a pure organic RTP material. With an average lifetime of 380 ms, the phosphorescence peak was observed at 500 nm upon excitation at 325 nm. PVA matrix prevents oxygen and intramolecular motions from efficiently quenching the triplet states of the aromatic carbonyl groups in the CDs, which were the source of the phosphorescence. The water-soluble, room-temperature phosphorescent (RTP) material is pure organic, biocompatible, and readily applied, particularly in the food and pharmaceutical industries. Its potential applications are time-resolved imaging, chemical, and biological sensing.

4.6. Electroluminescence.

Electroluminescence (EL) is a well-known property of semiconductor nanomaterials; therefore, it is not surprising that EL research with potential applications in electrochemical domains has been sparked by CQDs [138-140]. CQD-based light-emitting diodes (LEDs) have tunable driving currents that allow the emission colour to be altered. Under varying working voltages, color-switchable EL from the same CQDs was observed, spanning from blue to white.

Two ideas were proposed by the researchers to understand the luminescence process of CQDs: one centred on the edge effect caused by various surface irregularities, and the other on band-gap emitters in a conjoined p domain. The quantum-imprisonment effect of p-conjugated electrons within the sp2 atomic domain determines the PL properties of CQD fluorescence. This impact is modifiable by the conjugated p domain's scale, edge orientation, and shape. Fluorescence emission is caused by surface defects, such as hybridized carbon with sp2 and sp3 bonds, as well as additional surface irregularities in CQDs. The peak location and fluorescence emission are linked to this surface defect.

4.7. Chemiluminescence ~~[136-140]~~.

CQDs' Chemiluminescence (CL) exists together with oxidants like cerium (IV) and potassium permanganate ($KMnO_4$). According to electron paramagnetic resonance (EPR), oxidants such as cerium (IV) and KMnO4 can introduce holes into CQDs. This process accelerates electron-hole annihilation and increases the number of holes in CQDs, resulting in CL emission with the release of energy [136-140]. Moreover, CQD fixations in a specific reach affect the CL intensity. Raising the temperature also found a positive effect on the CL. The CL properties can be made by changing their surface properties. During the production of CQDs (NaOH or KOH), a noble CL phenomenon was seen in a highly alkaline solution. The CQDs demonstrated a high electron donor capacity towards dissolved oxygen in a NaOH solution, resulting in the formation of the superoxide anion radical (O^{2-}). These results directly confirmed the highest electron-donating potential of CQDs. The recombination rate of the injected high-energy carrier($e-$) via chemical reduction and temperature-related stimulation creates +ve charge carriers and has been ascribed to this performance in a non-acidic environment. It creates new opportunities for its application in reductive substance analysis. The combined properties of CQDs as an acceptor and donor of electrons provide great promise for optometry and catalysis.

4.8. Photo-induced electron transfer.

CQDs in solution are either electron donors or acceptors, suggesting that photo-induced CQDs are powerful electron donors and acceptors [141-146]. Even though the photo-induced electron-transfer characteristic of CQDs has received considerable attention. The charge dissociation in CQDs caused by photolysis has not yet been directly demonstrated. Certain indirect analytical proof was obtained by redox reactions. Photo-Induced Electron Transfer (PIET) characteristic was observed in photoluminescence decay tests of CQDs, employing the known electron donors N, N-diethylaniline and the acceptor 2, 4-dinitrotoluene. The important PIET characteristic of CQDs creates new opportunities for redox processes like light energy conversion and related applications. Further developed photo-induced electron and hole separation proficiency is the result of CQDs' effective capture of photo-generated electrons from semiconductors in compound photocatalysts. Furthermore, the redox-active character of photoexcited CQDs was demonstrated by reducing metal ions in aqueous solution. When a noble metal (silver, gold, or platinum) salt is added to the CQD water solution, it deposits the noble metal (silver, gold, or platinum) on the CQDs' exterior. Once again, radiative recombination is disrupted when the noble metal, being electron-affinitive, absorbs electrons from the connected CQDs, causing the fluorescence emissions.

5. Applications

There are various applications of CQDs in biomedical and optoelectronic areas.

5.1. Biomedical applications of CQDs.

The various biomedical applications of CQDs are given below (Figure 6). They demonstrate negligible cytotoxicity towards living cells and outstanding photo stability.

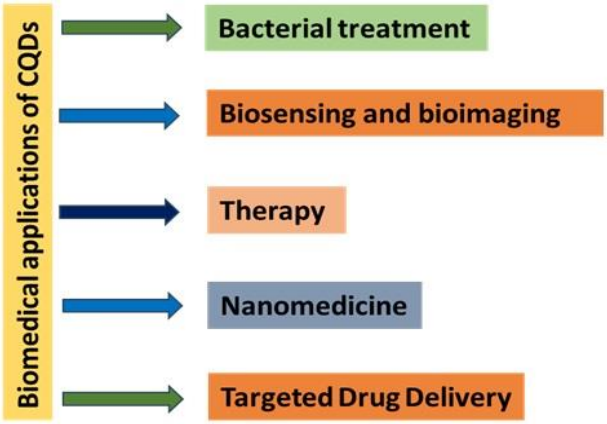

Figure 6. Various biomedical applications of CQDs.

5.1.1. Bacterial treatment.

Due to the severe health implications of bacterial infections, prompt diagnosis is necessary for effective clinical treatment. Furthermore, the search for potent bactericidal agents is required to reduce drug resistance and bacterial infections. Therefore, in the search for drug delivery methods for antibacterial applications, quaternary ammonium compounds (QACs) on nanoparticles (NPs) are of major interest [141-144]. It has been shown that nanoparticles offer a lot of promising treatment for bacterial infections. For instance, nanoparticles coupled with a drug via covalent or non-covalent interactions showed increased antibacterial activity. Additionally, this conjugation decreased the minimum inhibitory concentration (MIC) compared to the unconjugated (free) medication. However, these nanoparticles cannot provide both inhibition and detection simultaneously because they lack fluorescent properties. CQDs, on the other hand, mostly exhibit the blue or green region of their distinctive, excitation-dependent fluorescence emission feature. Additionally, certain functional CQDs with a multicolor fluorescence emission feature have been synthesised. CQDs are generally utilised with a fluorescence microscope to identify and count the number of bacterial cells in sewage water.

5.1.2. Biosensing and bioimaging.

Due to their biocompatibility, low toxicity, and luminescent properties in organic frameworks, CQDs can be used for bioimaging and biosensing applications [144-148]. Fluorescence microscopy imaging of CQD-treated human cell lines, the liver, and the kidneys of CQD-fed mice revealed outstanding fluorescence emission with extremely little cytotoxicity of CQDs. These were synthesized from the decomposition of citric acid monohydrate and diethylene glycol bis (3-aminopropyl). The bacterial DNA-derived DNA-CQD was taken up by the human kidney cell lines HEK 293. Furthermore, they were ingested by gram-negative and gram-positive bacteria. They were plainly observable by confocal microscopy. When

compared to a normal brain, CQD-Asp, which was produced by straightforward thermolysis of glucose and l-aspartic acid, was able to target gliomas and cross the blood-brain barrier precisely. As a result, CQD-Asp could serve as a fluorescent imaging agent for non-invasive brain glioma diagnosis, as it shows stronger selectivity for glioma cells than for normal brain cells. Another significant use of CQDs that makes use of their photoluminescence is biosensing. Conjugated quantum dots with organic dyes proved to be an efficient tool for H2S analysis. Within the sight of H2S, the blue discharge of CQD-natural color was changed to green. Under a fluorescent magnifying lens, CQD-natural colors could distinguish physiological levels of $H2S$ in the human cell lines HeLa and L929, with a shift from blue to green.

5.1.3. Therapy.

Diagnostics is a significant area in which CQDs are used in biomedicine [142-151]. Disease detection has been accomplished with the use of semiconductor quantum dots. CQDs are safer than traditional semiconductor quantum dots. Cl-CQDs are used to identify the desmin protein; patients with colorectal cancer had elevated serum levels of desmin. With great specificity and sensitivity, the CQD-based nanoscale probe may be employed to detect desmin in patient serum samples. CQDs are also able to differentiate between normal and cancerous cells. Glycerol and N-(3-(trimethoxysilyl)propyl) ethylenediamine were treated solvothermally to create silicon and N-doped CQD. Due to the reductive climate of threatening cells decreasing Fe^{3+} particles and causing a restoration of CQD luminescence, CQDs containing Fe^{3+} ions (CQDs/Fe^{3+}) help to find cancerous cells with the help of the ON and OFF process. FA-CQDs are allowed for the specific detection of cancer cells. The potential of CQD was demonstrated for the progression of point-of-care (POC) devices and inexpensive, efficient, and sensitive diagnostic nanoprobes. In addition, CQDs have been employed to develop microfluidic paper-based analytical instruments for identifying natural samples. POC diagnostic tools can help the inaccessible rural population in developing nations receive healthcare at a low cost of tests.

5.1.4. Nanomedicine.

Due to their low animal toxicity, CQDs—small fluorescent nanoparticles—offer a superior alternative to other fluorescent nanomaterials. As a result, they have significant applications in nanomedicine [145-148]. CQDs were given intravenously to mice as part of an experiment. After four weeks, an evaluation was conducted, and it was determined that there was no discernible impact on the organs' internal functions. Highly biocompatible CQDs do not alter thrombin activity in plasma samples. Moreover, these prevent blood from clotting. In photodynamic therapy, which is used to treat superficial tumours, CQDs have an appealing applicability. CQDs significantly inhibit MCF-7 and MDAMB-231 cancer cells. Furthermore, CQDs show photosensitizers. They are good candidates for photosensitization since they can create reactive oxygen species. CQDs localise selectively into tumours. The surface coating and the delivery route have an impact on the circulation and absorption of CQDs. When CQDs are injected, the body excretes them quickly and efficiently by intravenous, intramuscular, and subcutaneous injection. It has been used as photodynamic therapy to treat deep-seated tumors. Within the phototherapeutic window, excitation at 800 nm penetrates human tissue 4 times as deeply as stimulation at 630 nm, which has been used in clinical photodynamic therapy. It has additional applications in radiotherapy; PEG-CQDs can be coated with a silver shell to act as

radiosensitizers in Du145 cells (C-Ag-PEG CQDs). Due to nanoscale carriers, they are effective at tracking and delivering medications to genes. CQDs have a great deal of potential for gene delivery.

5.1.5. Targeted drug delivery.

Because of their biocompatibility, CQD are among the best C-based materials that can be utilized for different applications. CQDs have negligible cytotoxicity, which makes them promising options for focused, safe, and efficient distribution. Theranostic agents, or those with both therapeutic and diagnostic properties [145-151]. CQDs are appealing candidates when an anticancer medication (oxidised oxaliplatin) was formed. On the surface of CDs bearing amine groups, CD-Oxa was created. The therapeutic qualities of Oxa and the visual qualities of carbon dots are profitably combined in CD-Oxa. CQDs have superior biocompatibility, bioimaging capabilities, and anticancer effects. The in situ study shows that drug appropriation can be monitored by tracking CDOxa's fluorescence signal, which helps tailor the medication's dose and injection timing. An assembly was created by conjugating PEI-pDNA to CQDs and coupling the resulting conjugate to gold nanoparticles to transport DNA into cells. The experimental investigation demonstrated the possibility of cell delivery via CQDs. Gold nanorods functionalized with CQDs may enable the multimodal delivery of the anti-cancer drug doxorubicin. Haloperidol, an anti-psychotic, grafted CQD with cysteamine hydrochloride, can be utilised for regulated release for a maximum of 40 hours under physiological and Hixson-Crowell standard conditions. Together with bioimaging, ciprofloxacin, an expansive-spectrum antibiotic, and CQD conjugated under physiological conditions, resulted in a successful noble nanoscale carrier for targeted drug delivery.

5.2. Optoelectronic applications.

The emerging atomic-scale CQDs hold extraordinary promise for successful optoelectronic applications (Figure 7) due to their high surface area, unique optoelectronic properties such as strong, stable fluorescence, tunable band gaps, ultrafast electron extraction, and long hot-electron lifetimes [152-159].

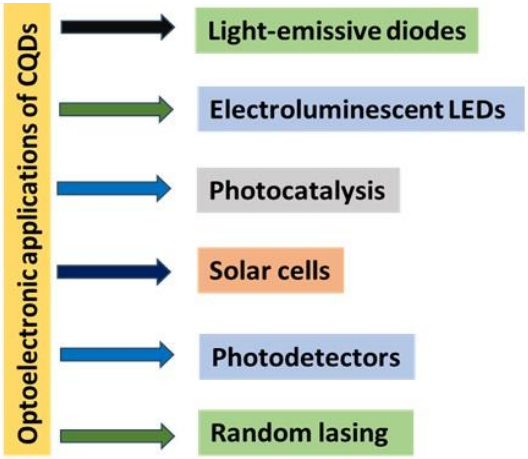

Figure 7. Various optoelectronic applications of CQDs.

5.2.1. Light-emissive diodes.

Light-emissive diodes (LEDs) are the upcoming generation of lighting sources for everyday use [160-164]. CQDs have all the earmarks of being an encouraging substitute for

costly phosphors derived from rare earth elements and hazardous metal-based semiconductors. CQDs are used in LED lighting as a noble type of fluorescent CQD system due to their inexpensive cost, no environmental impact, and adjustable steady fluorescence output. White LEDs (WLEDs) have emerged as a key energy-saving technology for our society's development because of their anticipated long-term stability, low power utilization, quick response time, and minimized size. CDs' large PL bandwidth makes them good candidates for WLED fabrication. According to the excitation mode, CD applications in LEDs can generally be split into two categories: optical and direct electrical. The former creates LEDs with a variety of transformations by using CDs as phosphors, whilst the latter creates LEDs using CDs' electroluminescence (EL).

5.2.2. Electroluminescent LEDs.

In recent years, Electroluminescent LEDs have grown rapidly due to CQDs' adjustable bandgap, superior solution-processability, low toxicity, and large-scale manufacturing [158-168]. Optoelectronic device efficiency is often poor due to excitation-dependent fluorescence quenching in CDs induced by surface defect states. As a result, bandgap emission CQD preparation is crucial. MCBFCQDs change from blue to red. These LEDs have an Lmax of 2050 cd m−2 and ongoing effectiveness of 1.1 cd A^{-1}, which is similar to that of semiconductor QD-based LEDs. To produce electroluminescence via radiative recombination, the MCBF-CQDs are immediately filled with electrons and holes, forming a functioning emission layer. With a narrow bandwidth of 30 nm, strong performance, a Lmax of 1882 to 4762 cd m^{-2}, and a current efficiency of 1.22 to 5.11 cd A^{-1}, the multicoloured LEDs based on NBE-T-CQDs exhibit high colour purity.

5.2.3. Photocatalysis.

The use of photocatalysis in natural synthesis has grown dramatically due to its environmental benefits [154-159, 160]. The ability of CQD solutions to suit extended wavelength light and energy conversion provides an excellent avenue for their application as photocatalysts in the natural synthesis process. CQDs in the size range of 1-4 nm are a powerful NIR light-driven photoactive material that can oxidise -OH into C6H5CHO with high conversion efficiency (92%) and specificity (100%). The photocatalytic activity of CQDs can be suitably modulated by doping and surface group fitting. CQDs with a size range of 5–10 nm, when mixed with graphite, exhibit light-induced protonation upon exposure to visible light. CQD nanocomposites promote the electrons' displacement from TiO_2. Due to the electrons' freedom to go along the CQDs' guiding paths, which allow for charge partitioning, correction, and blocking recombination, large holes were created at the TiO_2 surface. TiO_2 was empowered to deliver electron-opening frame pairs and significantly enhance photocatalytic activity with CQD-TiO_2. TiO_2 has been used to produce H2 through water splitting. A significant drawback to its photocatalytic proficiency is that it does not use enough visible light for lighting. The bulk TiO_2 bandgap lies in the UV region (3.0–3.2 eV), and TiO_2 absorbs less than 5% of solar radiation. Thus, one potential method to improve the performance of TiO_2 photocatalysts is by bandgap engineering via a potential modification of TiO_2-based media. With methyl blue (MB), it was shown that CQD-TiO_2 nanophase composites can completely degrade MB (50 mg/mL) in 25 minutes, with pure TiO_2 as a photocatalyst, degrading just 0.5% of the MB.

5.2.4. Solar cells.

The large range of light absorption of CQDs extends their use in solar cells (SCs). CQDs have been employed in a variety of SC, including silicon-based SCs, organic SCs, and dye-sensitized SCs [156-167]. In a conventional perovskite SC, a sub-monolayer of CQDs between the mesoporous titanium dioxide and perovskite layers was added. As a result, CQDs serve as a superfast scaffold to empower the halide perovskite's electron infusion into titanium dioxide. The accompanying SCs' photocurrent and power conversion efficiency (PCE) were significantly increased from 8.81% to 10.15%. These findings were obtained from transient absorption measurements, photocurrent–voltage curve analysis, and photocurrent quantum efficiency monitoring. CQDs were taken as a supplement to stabilise MAPbI3. Perovskite grain boundaries were passivated in order to further develop PCE from 17.59% to 18.81% and boost perovskite SC stability. Better optoelectronic characteristics and a reduced trap-state density could be induced by strong and stable contacts between the uncoordinated Pb in MAPbI3 and the -COOH, -OH, and -NH_2 gathering on the superficial level. Additionally, the interaction between MAPbI3 and CQDs created a shield to keep the perovskite out of the water to increase the stability of SCs. It is anticipated that CQDs will be a promising replacement for the hazardous elements (inorganic halide perovskites) that are generally used in solar cells.

5.2.5. Photodetectors.

Photo-generator transporters can be gathered and utilized in light detectors as a reverse process of electroluminescence [167-172]. The fundamental properties of photodetectors are the response band and responsivity of CQDs, which may usually be used for deep-UV photoluminescence and photodetection. An N-doped CQD-based broadband photodetector with interdigital gold electrodes was produced. It's interesting to note that under various light conditions, the CQD-based photosensors show photocurrent. This peculiarity can be made sense of by the free motion of photogenerated charge carrier pairs, which is impeded by the surface passivation of CQDs. When exposed to light, the bound excitons may catch transporters and make photoinduced charge traps. The negative photoresponse results from carriers being trapped when they pass through the CQDs. By implanting CQDs in a p-type sheet of graphene, photo detectors with high responsivity (0.2–0.5 A W^{-1}), high detectivity (41011 cm Hz1/2 W^{-1}), and an expansive range of reaction extend from visible to IR, were found. The device's photocurrent can be greatly increased at various voltages because of the charge carriers' tunnelling through the energy levels in CQDs. Gold (Au) and Silver (Ag) were mixed to create asymmetric electrodes for deep UV CQD-based photodetectors. Au functions as the anode and Ag as the cathode, resulting in easy separation of electrons and holes. Under forward bias, photogenerated transporters can drift uninhibitedly in the direction of the electrodes, and transporter recombination can be hindered.

5.2.6. Random lasing.

Random lasing is a low-limit irregular beam with single-colored and high intensity [166, 172-177]. There are many potential applications, including energy savings, biomedical therapy, military weaponry, and materials processing [175-178]. Furthermore, using brilliant multicolor fluorescent bandgap emission from CQDs, there is arbitrary lasing in blue, green, red, and white colours with a limit from 2.1 to 5.8 mJ/cm^2. Nonetheless, the substantial full-width at half maximum (FWHM) and the substantial Stokes shifts of the bandgap emission of CQDs unavoidably hinder the maintenance of population inversion and the conversion of

excitation energy into heat via the lifting strategy, thereby severely restricting further advancement. In order to leverage the potential of NBE-T-CQDs for highly efficient random lasers, very brilliant and spectral radiation of transmission capacity (FWHM of 29–30 nm) is required. Comparing blue, green, and red irregular light sources in contrast with cutting-edge perovskites and semiconductors, QD-based irregular lasing exhibits unexpectedly narrow FWHM of 0.9, 0.37, and 0.82 nm and low siphon limit of 0.087, 0.052, and 0.82 mJ cm^2. This occurred because NBE-T-CQDs have a very small FWHM, which makes it easier for the population to grow rapidly at low siphon energy thickness and for optical intensification to occur at low pump energy density.

6. Summary

In this work, numerous C-dot synthesis methods, characterization processes, optical properties, and various applications in biomedical and optoelectronic areas of CQDs are discussed. Even though a number of techniques have been used to synthesise CQDs, the exact sizes and well-defined structures remain scarce to explore. For specific applications and property studies, it is imperative to synthesize CQDs in an easy, environmentally friendly method with a predetermined size and structure. For both basic and practical applications, C-dots with synchronous visible, NIR, and up-conversion luminescence are highly desirable. These zero-dimensional carbon-based materials possess special optical properties, photo-stability, biocompatibility, water solubility, and low toxicity, making them suitable for a variety of applications. To prevent background and autofluorescence, CQD-driven biosensing and bioimaging need to be enhanced to become more discriminating and sensitive. Furthermore, CQDs have the potential to transform the domain of biomedicine, including nanomedicine, completely. Compared with perovskite and semiconductor quantum dots, CQDs offer advantages for biomedical and solar cell applications due to their non-toxic chemical composition and photochemical stability. In the biological pH range, the partly crystalline CQD exhibited robust, stable photoluminescence with both excitation-dependent and excitation-independent upconversion characteristics. The key challenges for CQD-based photocatalysts stem from limited understanding of mechanisms, inadequate control over doping and surface functionalization, and the lack of meticulous synthesis methods. In the future, integrating artificial intelligence and machine learning tools with advanced characterization techniques might enable scalable synthesis techniques and accurate property tuning.

Author Contributions

Conceptualization S.P., S.K.D., and B.D.; methodology, S.L. and K.M.; software, N.M.; validation, S.P., S.K.D., and B.D.; formal analysis, S.L. and K.M.; investigation, S.P. and B.D.; resources, S.L. and K.M.; writing—original draft preparation, S.P., S.L., and B.D.; writing—review and editing, S.K.D. and B.D.; visualization, S.L., S.P., N.M., and K.M.; supervision, S.K.D. and B.D. All authors have read and agreed to the published version of the manuscript.

Institutional Review Board Statement

Not applicable.

Informed Consent Statement

Not applicable.

Data Availability Statement

Data supporting the findings of this study are available upon reasonable request from the corresponding author.

Funding

This research received no external funding.

Acknowledgments

We are thankful to Dr. Bipin Bihari Swain, Professor (Retd.), Khallikote University, Odisha, for providing valuable inputs during the progress of the work.

Conflicts of Interest

The authors declare no conflict of interest.

Reference

1. Xie, Y.; Filchakova, O.; Yang, Q.; Yesbolatov, Y.; Tursynkhan, D.; Kassymbek, A.; Bouhrara, M.; Wang, K.; Balanay, M.; Fan, H. Inhibition of Cancer Cell Proliferation by Carbon Dots Derived from Date Pits at Low-Dose. *ChemistrySelect* **2017**, *2*, 4079-4083, https://doi.org/10.1002/slct.201700575.
2. Baig, M.B.; Al-Zahrani, K.H.; Schneider, F.; Straquadine, G.S.; Mourad, M. Food waste posing a serious threat to sustainability in the Kingdom of Saudi Arabia – A systematic review. *Saudi J. Biol. Sci.* **2019**, *26*, 1743-1752, https://doi.org/10.1016/j.sjbs.2018.06.004.
3. De Menna, F.; Dietershagen, J.; Loubiere, M.; Vittuari, M. Life cycle costing of food waste: A review of methodological approaches. *Waste Manag.* **2018**, *73*, 1-13, https://doi.org/10.1016/j.wasman.2017.12.032.
4. Hu, W.; Wang, T.; Yang, J. Tunable Schottky contacts in hybrid graphene–phosphorene nanocomposites. *J. Mater. Chem. C* **2015**, *3*, 4756-4761, https://doi.org/10.1039/C5TC00759C.
5. Kong, J.; Wei, Y.; Zhou, F.; Shi, L.; Zhao, S.; Wan, M.; Zhang, X. Carbon Quantum Dots: Properties, Preparation, and Applications. *Molecules* **2024**, *29*, 2002, https://doi.org/10.3390/molecules29092002.
6. Li, Y.; Hu, Y.; Zhao, Y.; Shi, G.; Deng, L.; Hou, Y.; Qu, L. An Electrochemical Avenue to Green-Luminescent Graphene Quantum Dots as Potential Electron-Acceptors for Photovoltaics. *Adv. Mater.* **2011**, *23*, 776-780, https://doi.org/10.1002/adma.201003819.
7. Cao, L.; Sahu, S.; Anilkumar, P.; Bunker, C.E.; Xu, J.; Fernando, K.A.S.; Wang, P.; Guliants, E.A.; Tackett, K.N., II; Sun, Y.-P. Carbon Nanoparticles as Visible-Light Photocatalysts for Efficient CO_2 Conversion and Beyond. *J. Am. Chem. Soc.* **2011**, *133*, 4754-4757, https://doi.org/10.1021/ja200804h.
8. Ozyurt, D.; Kobaisi, M.A.; Hocking, R.K.; Fox, B. Properties, synthesis, and applications of carbon dots: A review. *Carbon Trends* **2023**, *12*, 100276, https://doi.org/10.1016/j.cartre.2023.100276.
9. Kumar, P.; Dua, S.; Kaur, R.; Kumar, M.; Bhatt, G. A review on advancements in carbon quantum dots and their application in photovoltaics. *RSC Adv.* **2022**, *12*, 4714-4759, https://doi.org/10.1039/D1RA08452F.
10. Zuo, J.; Jiang, T.; Zhao, X.; Xiong, X.; Xiao, S.; Zhu, Z. Preparation and Application of Fluorescent Carbon Dots. *J. Nanomater.* **2015**, *2015*, 787862, https://doi.org/10.1155/2015/787862.
11. Liu, M.; Xu, Y.; Niu, F.; Gooding, J.J.; Liu, J. Carbon quantum dots directly generated from electrochemical oxidation of graphite electrodes in alkaline alcohols and the applications for specific ferric ion detection and cell imaging. *Analyst* **2016**, *141*, 2657-2664, https://doi.org/10.1039/C5AN02231B.
12. Alafeef, M.; Srivastava, I.; Aditya, T.; Pan, D. Carbon Dots: From Synthesis to Unraveling the Fluorescence Mechanism. *Small* **2024**, *20*, 2303937, https://doi.org/10.1002/smll.202303937.
13. Paulo, S.; Palomares, E.; Martinez-Ferrero, E. Graphene and Carbon Quantum Dot-Based Materials in Photovoltaic Devices: From Synthesis to Applications. *Nanomaterials* **2016**, *6*, 157, https://doi.org/10.3390/nano6090157.

14. Chae, A.; Choi, Y.; Jo, S.; Nur'aeni; Paoprasert, P.; Park, S.Y.; In, I. Microwave-assisted synthesis of fluorescent carbon quantum dots from an A_2/B_3 monomer set. *RSC Adv.* **2017**, *7*, 12663-12669, https://doi.org/10.1039/C6RA28176A.
15. Kaur, A.; Pandey, K.; Kaur, R.; Vashishat, N.; Kaur, M. Nanocomposites of Carbon Quantum Dots and Graphene Quantum Dots: Environmental Applications as Sensors. *Chemosensors* **2022**, *10*, 367, https://doi.org/10.3390/chemosensors10090367.
16. Sun, Y.-P.; Zhou, B.; Lin, Y.; Wang, W.; Fernando, K.A.S.; Pathak, P.; Meziani, M.J.; Harruff, B.A.; Wang, X.; Wang, H.; Luo, P.G.; Yang, H.; Kose, M.E.; Chen, B.; Veca, L.M.; Xie, S.-Y. Quantum-Sized Carbon Dots for Bright and Colorful Photoluminescence. *J. Am. Chem. Soc.* **2006**, *128*, 7756-7757, https://doi.org/10.1021/JA062677D.
17. Wang, X.; Feng, Y.; Dong, P.; Huang, J. A Mini Review on Carbon Quantum Dots: Preparation, Properties, and Electrocatalytic Application. *Front. Chem.* **2019**, *7*, 671, https://doi.org/10.3389/fchem.2019.00671.
18. Vibhute, A.; Patil, T.; Gambhir, R.; Tiwari, A.P. Fluorescent carbon quantum dots: Synthesis methods, functionalization and biomedical applications. *Appl. Surf. Sci. Advances* **2022**, *11*, 100311, https://doi.org/10.1016/j.apsadv.2022.100311.
19. Gonçalves, H.; Esteves da Silva, J.C.G. Fluorescent Carbon Dots Capped with PEG_{200} and Mercaptosuccinic Acid. *Journal of Fluorescence* **2010**, *20*, 1023-1028, https://doi.org/10.1007/s10895-010-0652-y.
20. Hu, S.; Liu, J.; Yang, J.; Wang, Y.; Cao, S. Laser synthesis and size tailor of carbon quantum dots. *J. Nanoparticle Res.* **2011**, *13*, 7247-7252, https://doi.org/10.1007/s11051-011-0638-y.
21. Zhi, B.; Yao, X.; Cui, Y.; Orr, G.; Haynes, C.L. Synthesis, applications and potential photoluminescence mechanism of spectrally tunable carbon dots. *Nanoscale* **2019**, *11*, 20411-20428, https://doi.org/10.1039/C9NR05028K.
22. Wang, L.; Ruan, F.; Lv, T.; Liu, Y.; Deng, D.; Zhao, S.; Wang, H.; Xu, S. One step synthesis of Al/N co-doped carbon nanoparticles With enhanced photoluminescence. *J. Luminesc.* **2015**, *158*, 1–5, https://doi.org/10.1016/j.jlumin.2014.09.029.
23. Singh, I.; Arora, R.; Dhiman, H.; Pahwa, R. Carbon quantum dots: Synthesis, characterization and biomedical applications. *Turk. J. Pharm. Sci* **2018**, *15*, 219-230, https://doi.org/10.4274/tjps.63497.
24. Arora, N.; Sharma, N.N. Arc discharge synthesis of carbon nanotubes: Comprehensive review. *Diam. Relat. Mater.* **2014**, *50*, 135-150, https://doi.org/10.1016/j.diamond.2014.10.001.
25. Zuo, P.; Lu, X.; Sun, Z.; Guo, Y.; He, H. A review on syntheses, properties, characterization and bioanalytical applications of fluorescent carbon dots. *Microchim. Acta* **2016**, *183*, 519-542, https://doi.org/10.1007/s00604-015-1705-3.
26. Chao-Mujica, F.J.; Garcia-Hernández, L.; Camacho-López, S.; Camacho-López, M.; Camacho-López, M.A.; Reyes Contreras, D.; Pérez-Rodríguez, A.; Peña-Caravaca, J.P.; Páez-Rodríguez, A.; Darias-Gonzalez, J.G.; Hernandez-Tabares, L.; Arias de Fuentes, O.; Prokhorov, E.; Torres-Figueredo, N.; Reguera, E.; Desdin-García, L.F. Carbon quantum dots by submerged arc discharge in water: Synthesis, characterization, and mechanism of formation. *J. Appl. Phys.* **2021**, *129*, 163301, https://doi.org/10.1063/5.0040322.
27. Dey, S.; Govindaraj, A.; Biswas, K.; Rao, C.N.R. Luminescence properties of boron and nitrogen doped graphene quantum dots prepared from arc-discharge-generated doped graphene samples. *Chem. Phys. Lett.* **2014**, *595-596*, 203-208, https://doi.org/10.1016/j.cplett.2014.02.012.
28. Li, H.; He, X.; Kang, Z.; Huang, H.; Liu, Y.; Liu, J.; Lian, S.; Tsang, C.H.A.; Yang, X.; Lee, S.T. Water-soluble fluorescent carbon quantum dots and photocatalyst design. *Angew. Chem. Int. Ed.* **2010**, *49*, 4430-4434, https://doi.org/10.1002/ange.200906154.
29. Li, X.; Zhao, Z.; Pan, C. Electrochemical exfoliation of carbon dots with the narrowest full width at half maximum in their fluorescence spectra in the ultraviolet region using only water as electrolyte. *Chem. Commun.* **2016**, *52*, 9406-9409, https://doi.org/10.1039/C6CC03080G.
30. Ran, Q.; Wang, X.; Ling, P.; Yan, P.; Xu, J.; Jiang, L.; Wang, Y.; Su, S.; Hu, S.; Xiang, J. A thermal-assisted electrochemical strategy to synthesize carbon dots with bimodal photoluminescence emission. *Carbon* **2022**, *193*, 404-411, https://doi.org/10.1016/j.carbon.2022.03.041.
31. Crista, D.M.A.; Esteves da Silva, J.C.G.; Pinto da Silva, L. Evaluation of Different Bottom-up Routes for the Fabrication of Carbon Dots. *Nanomaterials* **2020**, *10*, 1316, https://doi.org/10.3390/nano10071316.
32. Castañeda-Serna, H.U.; Calderón-Domínguez, G.; García-Bórquez, A.; Salgado-Cruz, M.d.l.P.; Farrera Rebollo, R.R. Structural and luminescent properties of CQDs produced by microwave and conventional

hydrothermal methods using pelagic Sargassum as carbon source. *Opt. Mater.* **2022**, *126*, 112156, https://doi.org/10.1016/j.optmat.2022.112156.

33. Zhang, B.; Liu, C.-y.; Liu, Y. A Novel One-Step Approach to Synthesize Fluorescent Carbon Nanoparticles. *Eur. J. Inorg. Chem.* **2010**, *2010*, 4411-4414, https://doi.org/10.1002/ejic.201000622.
34. Hong, Y.; Chen, X.; Zhang, Y.; Zhu, Y.; Sun, J.; Swihart, M.T.; Tan, K.; Dong, L. One-pot hydrothermal synthesis of high quantum yield orange-emitting carbon quantum dots for sensitive detection of perfluorinated compounds. *New J. Chem.* **2022**, *46*, 19658-19666, https://doi.org/10.1039/D2NJ02907C.
35. Huo, X.; Liu, L.; Bai, Y.; Qin, J.; Yuan, L.; Feng, F. Facile synthesis of yellowish-green emitting carbon quantum dots and their applications for phoxim sensing and cellular imaging. *Anal. Chim. Acta* **2022**, *1206*, 338685, https://doi.org/10.1016/j.aca.2021.338685.
36. Döring, A.; Ushakova, E.; Rogach, A.L. Chiral carbon dots: synthesis, optical properties, and emerging applications. *Light Sci. Appl.* **2022**, *11*, 75, https://doi.org/10.1038/s41377-022-00764-1.
37. Toma, E.E.; Stoian, G.; Cojocaru, B.; Parvulescu, V.I.; Coman, S.M. ZnO/CQDs Nanocomposites for Visible Light Photodegradation of Organic Pollutants. *Catalysts* **2022**, *12*, 952, https://doi.org/10.3390/catal12090952.
38. Lu, S.; Sui, L.; Wu, M.; Zhu, S.; Yong, X.; Yang, B. Graphitic Nitrogen and High-Crystalline Triggered Strong Photoluminescence and Room-Temperature Ferromagnetism in Carbonized Polymer Dots. *Adv. Sci.* **2019**, *6*, 1801192, https://doi.org/10.1002/advs.201801192.
39. Kapri, A.S.Z.; Nor, N.M.; Mohamed, A.R. Facile synthesis of Xerogel-embedded N/S/O-doped CQDs derived from oil palm mesocarp fiber for enhanced CO2 capture. *Sep. Purif. Technol.* **2026**, *386*, 136469, https://doi.org/10.1016/j.seppur.2025.136469.
40. Liu, C.; Zhang, P.; Tian, F.; Li, W.; Li, F.; Liu, W. One-step synthesis of surface passivated carbon nanodots by microwave assisted pyrolysis for enhanced multicolor photoluminescence and bioimaging. *J. Mater. Chem.* **2011**, *21*, 13163-13167, https://doi.org/10.1039/C1JM12744F.
41. Zhu, H.; Wang, X.; Li, Y.; Wang, Z.; Yang, F.; Yang, X. Microwave synthesis of fluorescent carbon nanoparticles with electrochemiluminescence properties. *Chem. Commun.* **2009**, 5118-5120, https://doi.org/10.1039/B907612C.
42. Liu, C.; Zhang, P.; Zhai, X.; Tian, F.; Li, W.; Yang, J.; Liu, Y.; Wang, H.; Wang, W.; Liu, W. Nano-carrier for gene delivery and bioimaging based on carbon dots with PEI-passivation enhanced fluorescence. *Biomaterials* **2012**, *33*, 3604-3613, https://doi.org/10.1016/j.biomaterials.2012.01.052.
43. Krishnamoorthy, K.; Veerapandian, M.; Mohan, R.; Kim, S.-J. Investigation of Raman and photoluminescence studies of reduced graphene oxide sheets. *Appl. Phys. A* **2012**, *106*, 501-506, https://doi.org/10.1007/s00339-011-6720-6.
44. Hegazy, M.; Ayad, M.M.; Ghali, M.; Ogi, T. Rapid microwave synthesis of licorice-derived carbon quantum dots as UV-blockers for food packaging applications. *Diam. Relat. Mater.* **2026**, *62*, 113291, https://doi.org/10.1016/j.diamond.2026.113291.
45. Ahlawat, A.; Rana, P.S.; Solanki, P.R. Studies of photocatalytic and optoelectronic properties of microwave synthesized and polyethyleneimine stabilized carbon quantum dots. *Mater. Lett.* **2021**, *305*, 130830, https://doi.org/10.1016/j.matlet.2021.130830.
46. Architha, N.; Ragupathi, M.; Shobana, C.; Selvankumar, T.; Kumar, P.; Lee, Y.S.; Kalai Selvan, R. Microwave-assisted green synthesis of fluorescent carbon quantum dots from *Mexican Mint* extract for Fe^{3+} detection and bio-imaging applications. *Environ. Res.* **2021**, *199*, 111263, https://doi.org/10.1016/j.envres.2021.111263.
47. Laddha, H.; Yadav, P.; Jain, Y.; Sharma, M.; Reza, M.; Agarwal, M.; Gupta, R. One-pot microwave-assisted synthesis of blue emissive multifunctional N-S-P co-doped carbon dots as a nanoprobe for sequential detection of Cr(VI) and ascorbic acid in real samples, fluorescent ink and logic gate operation. *J. Mol. Liq.* **2022**, *346*, 117088, https://doi.org/10.1016/j.molliq.2021.117088.
48. Bebas, P.K.; Larsson, M.A.; Ramachandran, P.; Jarujamrus, P.; Lee, H.L. Microwave synthesis of blue emissive N-doped carbon quantum dots as a fluorescent probe for free chlorine detection. *Sains Malays* **2022**, *51*, 1197-1212, http://doi.org/10.17576/jsm-2022-5104-20.
49. Jeong, G.; Lee, J.M.; Lee, J.A.; Praneerad, J.; Choi, C.A.; Supchocksoonthorn, P.; Roy, A.K.; Chae, W.-S.; Paoprasert, P.; Yeo, M.K.; Murali, G.; Park, S.Y.; Lee, D.-K.; In, I. Microwave-assisted synthesis of multifunctional fluorescent carbon quantum dots from A4/B2 polyamidation monomer sets. *Appl. Surf. Sci.* **2021**, *542*, 148471, https://doi.org/10.1016/j.apsusc.2020.148471.

50. Bourlinos, A.B.; Stassinopoulos, A.; Anglos, D.; Zboril, R.; Georgakilas, V.; Giannelis, E.P. Photoluminescent Carbogenic Dots. *Chem. Mater.* **2008**, *20*, 4539-4541, https://doi.org/10.1021/cm800506r.
51. Nazar, M.; Hasan, M.; Wirjosentono, B.; Gani, B.A.; Nada, C.E. Microwave Synthesis of Carbon Quantum Dots from Arabica Coffee Ground for Fluorescence Detection of Fe^{3+}, Pb^{2+}, and Cr^{3+}. *ACS Omega* **2024**, *9*, 20571-20581, https://doi.org/10.1021/acsomega.4c02254.
52. Zong, J.; Zhu, Y.; Yang, X.; Shen, J.; Li, C. Synthesis of photoluminescent carbogenic dots using mesoporous silica spheres as nanoreactors. *Chem. Commun.* **2011**, *47*, 764-766, https://doi.org/10.1039/C0CC03092A.
53. Shen, J.; Zhu, Y.; Yang, X.; Li, C. Graphene quantum dots: emergent nanolights for bioimaging, sensors, catalysis and photovoltaic devices. *Chem. Commun.* **2012**, *48*, 3686-3699, https://doi.org/10.1039/C2CC00110A.
54. LeCroy, G.E.; Wang, P.; Bunker, C.E.; Fernando, K.S.; Liang, W.; Ge, L.; Reibold, M.; Sun, Y.P. Hybrid carbon dots platform enabling opportunities for desired optical properties and redox characteristics by-design. *Chem. Phys. Lett.* **2019**, *724*, 8-12, https://doi.org/10.1016/j.cplett.2019.03.046.
55. Lu, W.; Qin, X.; Liu, S.; Chang, G.; Zhang, Y.; Luo, Y.; Asiri, A.M.; Al-Youbi, A.O.; Sun, X. Economical, Green Synthesis of Fluorescent Carbon Nanoparticles and Their Use as Probes for Sensitive and Selective Detection of Mercury(II) Ions. *Anal. Chem.* **2012**, *84*, 5351-5357, https://doi.org/10.1021/ac3007939.
56. Ameta, R.; Bhatt, J.P.; Ameta, S.C. Quantum Dots Fundamentals, Synthesis and Applications. Elsevier: **2023**; https://doi.org/10.1016/C2020-0-01037-6.
57. Wang, Z.; Changotra, R.; Dasog, M.; Singh Selopal, G.; Yang, J.; He, Q.S. Carbon quantum dots: Synthesis via hydrothermal processing, doping strategies, integration with photocatalysts, and their application in photocatalytic hydrogen production. *Sustain. Mater. Technol.* **2025**, *44*, e01386, https://doi.org/10.1016/j.susmat.2025.e01386.
58. Shen, T.; Wang, Q.; Guo, Z.; Kuang, J.; Cao, W. Hydrothermal synthesis of carbon quantum dots using different precursors and their combination with TiO_2 for enhanced photocatalytic activity. *Ceram. Int.* **2018**, *44*, 11828-11834, https://doi.org/10.1016/j.ceramint.2018.03.271.
59. Lin, Y.; Wang, L. Synthesis of Carbon Quantum Dots Based on Hydrothermal Method and Its Application. *Highl. Sci. Eng. Technol.* **2022**, *26*, 312-319, https://doi.org/10.54097/hset.v26i.3991.
60. Qin, X.; Lu, W.; Asiri, A.M.; Al-Youbi, A.O.; Sun, X. Microwave-assisted rapid green synthesis of photoluminescent carbon nanodots from flour and their applications for sensitive and selective detection of mercury(II) ions. *Sens. Actuators, B-Chem.* **2013**, *184*, 156-162, https://doi.org/10.1016/j.snb.2013.04.079.
61. Yuan, X.; Liu, Z.; Guo, Z.; Ji, Y.; Jin, M.; Wang, X. Cellular distribution and cytotoxicity of graphene quantum dots with different functional groups. *Nanoscale Res. Lett.* **2014**, *9*, 108, https://doi.org/10.1186/1556-276X-9-108.
62. Jiang, J.; He, Y.; Li, S.; Cui, H. Amino acids as the source for producing carbon nanodots: microwave assisted one-step synthesis, intrinsic photoluminescence property and intense chemiluminescence enhancement. *Chem. Commun.* **2012**, *48*, 9634-9636, https://doi.org/10.1039/C2CC34612E.
63. Yang, C.; He, X.; Chen, J.; Chen, D.; Liu, Y.; Xiong, F.; Shi, F.; Dou, J.; Gu, N. Fe_3O_4 nanoparticle loaded paclitaxel induce multiple myeloma apoptosis by cell cycle arrest and increase cleavage of caspases in vitro. *J. Nanoparticle Res.* **2013**, *15*, 1840, https://doi.org/10.1007/s11051-013-1840-x.
64. Iqbal, Q.; Habib, M.; Alzaid, M.; Khan, M.T.; Tho, P.T.; Ahmad, P.; Shah, Y.A. Synthesis and investigation of electromechanical property of lead-free BiFeO3–BaTiO3 quenched ceramics. *J. Mater. Sci.: Mater. Electron.* **2023**, *34*, 404, https://doi.org/10.1007/s10854-023-09837-2.
65. Hsu, P.-C.; Chang, H.-T. Synthesis of high-quality carbon nanodots from hydrophilic compounds: role of functional groups. *Chem. Commun.* **2012**, *48*, 3984-3986, https://doi.org/10.1039/C2CC30188A.
66. Hsu, P.-C.; Chen, P.-C.; Ou, C.-M.; Chang, H.-Y.; Chang, H.-T. Extremely high inhibition activity of photoluminescent carbon nanodots toward cancer cells. *J. Mater. Chem. B* **2013**, *1*, 1774-1781, https://doi.org/10.1039/C3TB00545C.
67. Bao, L.; Zhang, Z.-L.; Tian, Z.-Q.; Zhang, L.; Liu, C.; Lin, Y.; Qi, B.; Pang, D.-W. Electrochemical Tuning of Luminescent Carbon Nanodots: From Preparation to Luminescence Mechanism. *Adv. Mater.* **2011**, *23*, 5801-5806, https://doi.org/10.1002/adma.201102866.
68. Tarannum, N.; Pooja, K.; Singh, M.; Panwar, A. A study on the development of C-dots via green chemistry: a state-of-the-art review. *Carbon Lett.* **2024**, *34*, 1537-1568, https://doi.org/10.1007/s42823-024-00742-0.

69. Zhang, M.; Bai, L.; Shang, W.; Xie, W.; Ma, H.; Fu, Y.; Fang, D.; Sun, H.; Fan, L.; Han, M.; Liu, C.; Yang, S. Facile synthesis of water-soluble, highly fluorescent graphene quantum dots as a robust biological label for stem cells. *J. Mater. Chem.* **2012**, *22*, 7461-7467, https://doi.org/10.1039/C2JM16835A.
70. Shinde, D.B.; Pillai, V.K. Electrochemical Preparation of Luminescent Graphene Quantum Dots from Multiwalled Carbon Nanotubes. *Chem. Eur. J.* **2012**, *18*, 12522-12528, https://doi.org/10.1002/chem.201201043.
71. Thambiraj, S.; Ravi Shankaran, D. Green synthesis of highly fluorescent carbon quantum dots from sugarcane bagasse pulp. *Appl. Surf. Sci.* **2016**, *390*, 435-443, https://doi.org/10.1016/j.apsusc.2016.08.106.
72. Bourlinos, A.B.; Stassinopoulos, A.; Anglos, D.; Zboril, R.; Karakassides, M.; Giannelis, E.P. Surface Functionalized Carbogenic Quantum Dots. *Small* **2008**, *4*, 455-458, https://doi.org/10.1002/smll.200700578.
73. Zhao, C.; Li, W.; Liang, Y.; Tian, Y.; Zhang, Q. Synthesis of BiOBr/carbon quantum dots microspheres with enhanced photoactivity and photostability under visible light irradiation. *Appl. Catal. A Gen.* **2016**, *527*, 127-136, https://doi.org/10.1016/j.apcata.2016.09.005.
74. Liu, R.; Wu, D.; Feng, X.; Müllen, K. Bottom-Up Fabrication of Photoluminescent Graphene Quantum Dots with Uniform Morphology. *J. Am. Chem. Soc.* **2011**, *133*, 15221-15223, https://doi.org/10.1021/ja204953k.
75. Mao, L.-H.; Tang, W.-Q.; Deng, Z.-Y.; Liu, S.-S.; Wang, C.-F.; Chen, S. Facile Access to White Fluorescent Carbon Dots toward Light-Emitting Devices. *Ind. Eng. Chem. Res.* **2014**, *53*, 6417-6425, https://doi.org/10.1021/ie500602n.
76. Roy, P.; Chen, P.-C.; Periasamy, A.P.; Chen, Y.-N.; Chang, H.-T. Photoluminescent carbon nanodots: synthesis, physicochemical properties and analytical applications. *Mater. Today* **2015**, *18*, 447-458, https://doi.org/10.1016/j.mattod.2015.04.005.
77. Peng, J.; Gao, W.; Gupta, B.K.; Liu, Z.; Romero-Aburto, R.; Ge, L.; Song, L.; Alemany, L.B.; Zhan, X.; Gao, G.; Vithayathil, S.A.; Kaipparettu, B.A.; Marti, A.A.; Hayashi, T.; Zhu, J.-J.; Ajayan, P.M. Graphene Quantum Dots Derived from Carbon Fibers. *Nano Lett.* **2012**, *12*, 844-849, https://doi.org/10.1021/nl2038979.
78. Tian, L.; Ghosh, D.; Chen, W.; Pradhan, S.; Chang, X.; Chen, S. Nanosized Carbon Particles From Natural Gas Soot. *Chem. Mater.* **2009**, *21*, 2803-2809, https://doi.org/10.1021/cm900709w.
79. Li, H.; He, X.; Liu, Y.; Yu, H.; Kang, Z.; Lee, S.-T. Synthesis of fluorescent carbon nanoparticles directly from active carbon via a one-step ultrasonic treatment. *Mater. Res. Bull.* **2011**, *46*, 147-151, https://doi.org/10.1016/j.materresbull.2010.10.013.
80. Wang, F.; Xie, Z.; Zhang, H.; Liu, C.-y.; Zhang, Y.-g. Highly Luminescent Organosilane-Functionalized Carbon Dots. *Adv. Funct. Mater.* **2011**, *21*, 1027-1031, https://doi.org/10.1002/adfm.201002279.
81. Anum, J.; Akhtar, M.A.; Khan, A.M.; Ahmed, K.; Sayes, C.M.; Almajwal, A.M.; Iqbal, J.; Rahim, A. Green-synthesized amino-rich carbon quantum dots: A dual-function platform for fluorescent detection of heavy metals and degradation of malachite green dye. *J. Water Process. Eng.* **2025**, *77*, 108472, https://doi.org/10.1016/j.jwpe.2025.108472.
82. Montazeri, F.; Baharfar, R.; Maleki, B. Ugi-Functionalized Magnetic Carbon Quantum Dots: an Efficient and Environmentally Friendly Catalyst for the Synthesis of 1,4-Dihydropyridines. *J. Sci.: Adv. Mater. Dev*. **2025**, *10*, 100958, https://doi.org/10.1016/j.jsamd.2025.100958.
83. Dong, Y.; Shao, J.; Chen, C.; Li, H.; Wang, R.; Chi, Y.; Lin, X.; Chen, G. Blue luminescent graphene quantum dots and graphene oxide prepared by tuning the carbonization degree of citric acid. *Carbon* **2012**, *50*, 4738-4743, https://doi.org/10.1016/j.carbon.2012.06.002.
84. Tang, L.; Ji, R.; Cao, X.; Lin, J.; Jiang, H.; Li, X.; Teng, K.S.; Luk, C.M.; Zeng, S.; Hao, J.; Lau, S.P. Deep Ultraviolet Photoluminescence of Water-Soluble Self-Passivated Graphene Quantum Dots. *ACS Nano* **2012**, *6*, 5102-5110, https://doi.org/10.1021/nn300760g.
85. Wang, Y.; Hu, A. Carbon quantum dots: synthesis, properties and applications. *J. Mater. Chem. C* **2014**, *2*, 6921-6939, https://doi.org/10.1039/C4TC00988F.
86. Qu, Y.; Li, X.; Zhang, H.; Huang, R.; Qi, W.; Su, R.; He, Z. Controllable synthesis of a sponge-like Z-scheme N,S-CQDs/Bi_2MoO_6@TiO_2 film with enhanced photocatalytic and antimicrobial activity under visible/NIR light irradiation. *J. Hazard. Mater.* **2022**, *429*, 128310, https://doi.org/10.1016/j.jhazmat.2022.128310.

87. Chang, K.; Zhu, Q.; Qi, L.; Guo, M.; Gao, W.; Gao, Q. Synthesis and Properties of Nitrogen-Doped Carbon Quantum Dots Using Lactic Acid as Carbon Source. *Materials* **2022**, *15*, 466, https://doi.org/10.3390/ma15020466.
88. Henriquez, G.; Ahlawat, J.; Fairman, R.; Narayan, M. Citric Acid-Derived Carbon Quantum Dots Attenuate Paraquat-Induced Neuronal Compromise In Vitro and In Vivo. *ACS Chem. Neurosci.* **2022**, *13*, 2399-2409, https://doi.org/10.1021/acschemneuro.2c00099.
89. Nammahachak, N.; Aup-Ngoen, K.K.; Asanithi, P.; Horpratum, M.; Chuangchote, S.; Ratanaphan, S.; Surareungchai, W. Hydrothermal synthesis of carbon quantum dots with size tunability via heterogeneous nucleation. *RSC Adv.* **2022**, *12*, 31729-31733, https://doi.org/10.1039/D2RA05989D.
90. Jamila, G.S.; Sajjad, S.; Leghari, S.A.K.; Kallio, T.; Flox, C. Glucose derived carbon quantum dots on tungstate-titanate nanocomposite for hydrogen energy evolution and solar light catalysis. *J. Nanostructure Chem.* **2021**, *12*, 611–623, https://doi.org/10.1007/s40097-021-00433-6.
91. Qiu, Y.; Li, D.; Li, Y.; Ma, X.; Li, J. Green carbon quantum dots from sustainable lignocellulosic biomass and its application in the detection of Fe^{3+}. *Cellulose* **2022**, *29*, 367-378, https://doi.org/10.1007/s10570-021-04314-7.
92. Kundu, A.; Maity, B.; Basu, S. Rice Husk-Derived Carbon Quantum Dots-Based Dual-Mode Nanoprobe for Selective and Sensitive Detection of Fe^{3+} and Fluoroquinolones. *ACS Biomater. Sci. Eng.* **2022**, *8*, 4764-4776, https://doi.org/10.1021/acsbiomaterials.2c00798.
93. El-brolsy, H.M.; Hanafy, N.A.N.; El-Kemary, M.A. Fighting Non-Small Lung Cancer Cells Using Optimal Functionalization of Targeted Carbon Quantum Dots Derived from Natural Sources Might Provide Potential Therapeutic and Cancer Bio Image Strategies. *Int. J. Mol. Sci.* **2022**, *23*, 13283, https://doi.org/10.3390/ijms232113283.
94. Kumari, M.; Chaudhary, G.R.; Chaudhary, S.; Umar, A.; Akbar, S.; Baskoutas, S. Bio-Derived Fluorescent Carbon Dots: Synthesis, Properties and Applications. *Molecules* **2022**, *27*, 5329, https://doi.org/10.3390/molecules27165329.
95. Yao, L.; Zhao, M.-M.; Luo, Q.-W.; Zhang, Y.-C.; Liu, T.-T.; Yang, Z.; Liao, M.; Tu, P.; Zeng, K.-W. Carbon Quantum Dots-Based Nanozyme from Coffee Induces Cancer Cell Ferroptosis to Activate Antitumor Immunity. *ACS Nano* **2022**, *16*, 9228-9239, https://doi.org/10.1021/acsnano.2c01619.
96. Yuan, F.; Li, S.; Fan, Z.; Meng, X.; Fan, L.; Yang, S. Shining carbon dots: Synthesis and biomedical and optoelectronic applications. *Nano Today* **2016**, *11*, 565-586, https://doi.org/10.1016/j.nantod.2016.08.006.
97. Liu, J.; Li, R.; Yang, B. Carbon Dots: A New Type of Carbon-Based Nanomaterial with Wide Applications. *ACS Cent. Sci.* **2020**, *6*, 2179-2195, https://doi.org/10.1021/acscentsci.0c01306.
98. Pan, D.; Zhang, J.; Li, Z.; Wu, M. Hydrothermal Route for Cutting Graphene Sheets into Blue-Luminescent Graphene Quantum Dots. *Adv. Mater.* **2010**, *22*, 734-738, https://doi.org/10.1002/adma.200902825.
99. Praseetha, P.K.; Litany, R.I.J.; Alharbi, H.M.; Khojah, A.A.; Akash, S.; Bourhia, M.; Mengistie, A.A.; Shazly, G.A. Green synthesis of highly fluorescent carbon quantum dots from almond resin for advanced theranostics in biomedical applications. *Sci. Rep.* **2024**, *14*, 24435, https://doi.org/10.1038/s41598-024-75333-0.
100. Qu, D.; Zheng, M.; Du, P.; Zhou, Y.; Zhang, L.; Li, D.; Tan, H.; Zhao, Z.; Xie, Z.; Sun, Z. Highly luminescent S, N co-doped graphene quantum dots with broad visible absorption bands for visible light photocatalysts. *Nanoscale* **2013**, *5*, 12272-12277, https://doi.org/10.1039/C3NR04402E.
101. Zhu, S.; Zhang, J.; Tang, S.; Qiao, C.; Wang, L.; Wang, H.; Liu, X.; Li, B.; Li, Y.; Yu, W.; Wang, X.; Sun, H.; Yang, B. Surface Chemistry Routes to Modulate the Photoluminescence of Graphene Quantum Dots: From Fluorescence Mechanism to Up-Conversion Bioimaging Applications. *Adv. Funct. Mater.* **2012**, *22*, 4732-4740, https://doi.org/10.1002/adfm.201201499.
102. Das, S.; Mondal, S.; Ghosh, D. Carbon quantum dots in bioimaging and biomedicines. *Front. Bioeng. Biotechnol.* **2024**, *11*, 1333752, https://doi.org/10.3389/fbioe.2023.1333752.
103. Li, L.; Dong, T. Photoluminescence tuning in carbon dots: surface passivation or/and functionalization, heteroatom doping. *J. Mater. Chem. C* **2018**, *6*, 7944-7970, https://doi.org/10.1039/C7TC05878K.
104. Peng, H.; Travas-Sejdic, J. Simple Aqueous Solution Route to Luminescent Carbogenic Dots from Carbohydrates. *Chem. Mater.* **2009**, *21*, 5563-5565, https://doi.org/10.1021/cm901593y.
105. Dimos, K. Carbon Quantum Dots: Surface Passivation and Functionalization. *Curr. Organic Chem.* **2016**, *20*, 682-695, https://doi.org/10.2174/1385272819666150730220948.

106. Kandasamy, G. Recent Advancements in Doped/Co-Doped Carbon Quantum Dots for Multi-Potential Applications. *C* **2019**, *5*, 24, https://doi.org/10.3390/c5020024.
107. Carolan, D.; Rocks, C.; Padmanaban, D.B.; Maguire, P.; Svrcek, V.; Mariotti, D. Environmentally friendly nitrogen-doped carbon quantum dots for next generation solar cells. *Sustain. Energy Fuels* **2017**, *1*, 1611-1619, https://doi.org/10.1039/C7SE00158D.
108. Gao, R.; Wu, Z.; Wang, L.; Liu, J.; Deng, Y.; Xiao, Z.; Fang, J.; Liang, Y. Green Preparation of Fluorescent Nitrogen-Doped Carbon Quantum Dots for Sensitive Detection of Oxytetracycline in Environmental Samples. *Nanomaterials* **2020**, *10*, 1561, https://doi.org/10.3390/nano10081561.
109. Yu, J.; Liu, C.; Yuan, K.; Lu, Z.; Cheng, Y.; Li, L.; Zhang, X.; Jin, P.; Meng, F.; Liu, H. Luminescence Mechanism of Carbon Dots by Tailoring Functional Groups for Sensing Fe^{3+} Ions. *Nanomaterials* **2018**, *8*, 233, https://doi.org/10.3390/nano8040233.
110. Zuo, G.; Xie, A.; Li, J.; Su, T.; Pan, X.; Dong, W. Large Emission Red-Shift of Carbon Dots by Fluorine Doping and Their Applications for Red Cell Imaging and Sensitive Intracellular Ag^{+} Detection. *J. Phys. Chem. C* **2017**, *121*, 26558-26565, https://doi.org/10.1021/acs.jpcc.7b10179.
111. Adedokun, O.; Roy, A.; Awodugba, A.O.; Devi, P.S. Fluorescent carbon nanoparticles from *Citrus sinensis* as efficient sorbents for pollutant dyes. *Luminescence* **2017**, *32*, 62-70, https://doi.org/10.1002/bio.3149.
112. Zhu, S.; Meng, Q.; Wang, L.; Zhang, J.; Song, Y.; Jin, H.; Zhang, K.; Sun, H.; Wang, H.; Yang, B. Highly photoluminescent carbon dots for multicolor patterning, sensors, and bioimaging. *Angew. Chem. Int. Ed.* **2013**, *152*, 4045-4049, https://doi.org/10.1002/ange.201300519.
113. Li, X.; Wang, H.; Shimizu, Y.; Pyatenko, A.; Kawaguchi, K.; Koshizaki, N. Preparation of carbon quantum dots with tunable photoluminescence by rapid laser passivation in ordinary organic solvents. *Chem. Commun.* **2011**, *47*, 932-934, https://doi.org/10.1039/C0CC03552A.
114. Sun, C.; Zhang, Y.; Kalytchuk, S.; Wang, Y.; Zhang, X.; Gao, W.; Zhao, J.; Cepe, K.; Zboril, R.; Yu, W.W.; Rogach, A.L. Down-conversion monochromatic light-emitting diodes with the color determined by the active layer thickness and concentration of carbon dots. *J. Mater. Chem. C* **2015**, *3*, 6613-6615, https://doi.org/10.1039/C5TC01379H.
115. Wang, R.; Wang, X.; Sun, Y. One-step synthesis of self-doped carbon dots with highly photoluminescence as multifunctional biosensors for detection of iron ions and pH. *Sens. Actuators B-Chem.* **2017**, *241*, 73-79, https://doi.org/10.1016/j.snb.2016.10.043.
116. Shen, J.; Zhu, Y.; Chen, C.; Yang, X.; Li, C. Facile preparation and upconversion luminescence of graphene quantum dots. *Chem. Commun.* **2011**, *47*, 2580-2582, https://doi.org/10.1039/C0CC04812G.
117. Yuan, T.; Meng, T.; He, P.; Shi, Y.; Li, Y.; Li, X.; Fan, L.; Yang, S. Carbon quantum dots: an emerging material for optoelectronic applications. *J. Mater. Chem. C* **2019**, *7*, 6820-6835, https://doi.org/10.1039/C9TC01730E.
118. Wang, Y.; Kalytchuk, S.; Zhang, Y.; Shi, H.; Kershaw, S.V.; Rogach, A.L. Thickness-Dependent Full-Color Emission Tunability in a Flexible Carbon Dot Ionogel. *J. Phys. Chem. Lett.* **2014**, *5*, 1412-1420, https://doi.org/10.1021/jz5005335.
119. Gao, M.X.; Liu, C.F.; Wu, Z.L.; Zeng, Q.L.; Yang, X.X.; Wu, W.B.; Li, Y.F.; Huang, C.Z. A surfactant-assisted redox hydrothermal route to prepare highly photoluminescent carbon quantum dots with aggregation-induced emission enhancement properties. *Chem. Commun.* **2013**, *49*, 8015-8017, https://doi.org/10.1039/C3CC44624G.
120. Serag, A.; Algarni, M.A.; Maksoud, A.A.A.A.; Alsulami, F.T.; Alatwi, E.S.; Alaqel, S.I.; Aljameeli, A.M.; Almalki, A.H. A novel spectrofluorimetric method for sensitive detection of homovanillic acid based on Zn-assisted N-CQDs fluorescence quenching: application in depression biomarker analysis. *J. Photoch. Photobio. A.* **2026**, *471*, 116730, https://doi.org/10.1016/j.jphotochem.2025.116730.
121. Chien, C.-T.; Li, S.-S.; Lai, W.-J.; Yeh, Y.-C.; Chen, H.-A.; Chen, I.S.; Chen, L.-C.; Chen, K.-H.; Nemoto, T.; Isoda, S.; Chen, M.; Fujita, T.; Eda, G.; Yamaguchi, H.; Chhowalla, M.; Chen, C.-W. Tunable Photoluminescence from Graphene Oxide. *Angew. Chem. Int. Ed.* **2012**, *51*, 6662-6666, https://doi.org/10.1002/anie.201200474.
122. Hu, S.; Trinchi, A.; Atkin, P.; Cole, I. Tunable Photoluminescence Across the Entire Visible Spectrum from Carbon Dots Excited by White Light. *Angew. Chem. Int. Ed.* **2015**, *54*, 2970-2974, https://doi.org/10.1002/anie.201411004.

123. Zhu, C.; Zhai, J.; Dong, S. Bifunctional fluorescent carbon nanodots: green synthesis via soy milk and application as metal-free electrocatalysts for oxygen reduction. *Chem. Commun.* **2012**, *48*, 9367-9369, https://doi.org/10.1039/C2CC33844K.
124. Tan, X.; Li, Y.; Li, X.; Zhou, S.; Fan, L.; Yang, S. Electrochemical synthesis of small-sized red fluorescent graphene quantum dots as a bioimaging platform. *Chem. Commun.* **2015**, *51*, 2544-2546, https://doi.org/10.1039/C4CC09332A.
125. Barakat, N.T.; El-Aziz, H.A.; Eid, M.I.; Ibrahim, F.A. Novel and Ultra-sensitive Harnessing of Native Fluorescence and Bio-Inspired N, S-CQDs: A Greener Path to Pharmaceutical and Biological Analysis of Moexipril with Enhanced Sustainability Profiles. *Talanta* **2025**, *12*, 100516, https://doi.org/10.1016/j.talo.2025.100516.
126. Eda, G.; Lin, Y.-Y.; Mattevi, C.; Yamaguchi, H.; Chen, H.-A.; Chen, I.S.; Chen, C.-W.; Chhowalla, M. Blue Photoluminescence from Chemically Derived Graphene Oxide. *Adv. Mater.* **2010**, *22*, 505-509, https://doi.org/10.1002/adma.200901996.
127. Sk, M.A.; Ananthanarayanan, A.; Huang, L.; Lim, K.H.; Chen, P. Revealing the tunable photoluminescence properties of graphene quantum dots. *J. Mater. Chem. C* **2014**, *2*, 6954-6960, https://doi.org/10.1039/C4TC01191K.
128. Xiao, L.; Chen, Z.; Qu, B.; Luo, J.; Kong, S.; Gong, Q.; Kido, J. Recent Progresses on Materials for Electrophosphorescent Organic Light-Emitting Devices. *Adv. Mater.* **2011**, *23*, 926-952, https://doi.org/10.1002/adma.201003128.
129. Ding, C.; Zhu, A.; Tian, Y. Functional Surface Engineering of C-Dots for Fluorescent Biosensing and in Vivo Bioimaging. *Acc. Chem. Res.* **2014**, *47*, 20-30, https://doi.org/10.1021/ar400023s.
130. Deka, M.J.; Chowdhury, D.; Nath, B.K. Recent development of modified fluorescent carbon quantum dots-based fluorescence sensors for food quality assessment. *Carbon Lett.* **2022**, *32*, 1131-1149, https://doi.org/10.1007/s42823-022-00347-5.
131. Zhang, H.; Huang, H.; Ming, H.; Li, H.; Zhang, L.; Liu, Y.; Kang, Z. Carbon quantum dots/Ag_3PO_4 complex photocatalysts with enhanced photocatalytic activity and stability under visible light. *J. Mater. Chem.* **2012**, *22*, 10501-10506, https://doi.org/10.1039/c2jm30703k.
132. Xia, J.; Di, J.; Li, H.; Xu, H.; Li, H.; Guo, S. Ionic liquid-induced strategy for carbon quantum dots/BiOX (X=Br, Cl) hybrid nanosheets with superior visible light-driven photocatalysis. *Appl. Catal. B-Environ.* **2016**, *181*, 260-269, https://doi.org/10.1016/j.apcatb.2015.07.035.
133. Ma, X.; Zeng, M.; Yang, X.; Huang, F.; Li, L.; Cheng, Z. A novel “off-on” ratiometric fluorescent probe based on nitrogen-doped carbon dots for silver ion and glutathione assays. *Talanta* **2026**, *296*, 128447, https://doi.org/10.1016/j.talanta.2025.128447.
134. Mintz, K.J.; Guerrero, B.; Leblanc, R.M. Photoinduced Electron Transfer in Carbon Dots with Long-Wavelength Photoluminescence. *J. Phys. Chem. C* **2018**, *122*, 29507-29515, https://doi.org/10.1021/acs.jpcc.8b06868.
135. Tan, J.; Zou, R.; Zhang, J.; Li, W.; Zhang, L.; Yue, D. Large-scale synthesis of N-doped carbon quantum dots and their phosphorescence properties in a polyurethane matrix. *Nanoscale* **2016**, *8*, 4742-4747, https://doi.org/10.1039/C5NR08516K.
136. Lin, Z.; Xue, W.; Chen, H.; Lin, J.-M. Classical oxidant induced chemiluminescence of fluorescent carbon dots. *Chem. Commun.* **2012**, *48*, 1051-1053, https://doi.org/10.1039/C1CC15290D.
137. Zhao, L.; Di, F.; Wang, D.; Guo, L.-H.; Yang, Y.; Wan, B.; Zhang, H. Chemiluminescence of carbon dots under strong alkaline solutions: a novel insight into carbon dot optical properties. *Nanoscale* **2013**, *5*, 2655-2658, https://doi.org/10.1039/C3NR00358B.
138. Xu, J.; Miao, Y.; Zheng, J.; Yang, Y.; Liu, X. Ultrahigh Brightness Carbon Dot–Based Blue Electroluminescent LEDs by Host–Guest Energy Transfer Emission Mechanism. *Adv. Opt. Mater.* **2018**, *6*, 1800181, https://doi.org/10.1002/adom.201800181.
139. Ahangari, A.; Salouti, M.; Heidari, Z.; Kazemizadeh, A.R.; Safari, A.A. Development of gentamicin-gold nanospheres for antimicrobial drug delivery to *Staphylococcal* infected foci. *Drug Deliv.* **2013**, *20*, 34-39, https://doi.org/10.3109/10717544.2012.746402.
140. Mandal, T.K.; Parvin, N. Rapid Detection of Bacteria by Carbon Quantum Dots. *J. Biomed. Nanotechnol.* **2011**, *7*, 846-848, https://doi.org/10.1166/jbn.2011.1344.
141. Ghacham, S.E.; Hejji, L.; Ali, Y.A.E.H.; Wahby, A.; Tamegart, L.; Pérez-Villarejo, L.; Mennane, Z.; Souhail, B.; Azzouz, A. Enhanced antibacterial and wound healing efficacy of a novel

CQDs@AgNPs@CS-based nanocomposites: A multifunctional approach for advanced wound care. *Int. J. Biol. Macromol.* **2025**, *311*, 143621, https://doi.org/10.1016/j.ijbiomac.2025.143621.

142. Liu, X.; Zhang, N.; Bing, T.; Shangguan, D. Carbon Dots Based Dual-Emission Silica Nanoparticles as a Ratiometric Nanosensor for Cu^{2+}. *Anal. Chem.* **2014**, *86*, 2289-2296, https://doi.org/10.1021/ac404236y.
143. Shamsipur, M.; Molaei, K.; Molaabasi, F.; Hosseinkhani, S.; Alizadeh, N.; Alipour, M.; Moassess, S. One-step synthesis and characterization of highly luminescent nitrogen and phosphorus co-doped carbon dots and their application as highly selective and sensitive nanoprobes for low level detection of uranyl ion in hair and water samples and application to cellular imaging. *Sens. Actuators B-Chem.* **2018**, *257*, 772-782, https://doi.org/10.1016/j.snb.2017.11.018.
144. Posthuma-Trumpie, G.A.; Wichers, J.H.; Koets, M.; Berendsen, L.B.J.M.; van Amerongen, A. Amorphous carbon nanoparticles: a versatile label for rapid diagnostic (immuno)assays. *Anal. BioAnal. Chem.* **2012**, *402*, 593-600, https://doi.org/10.1007/s00216-011-5340-5.
145. Havrdova, M.; Hola, K.; Skopalik, J.; Tomankova, K.; Petr, M.; Cepe, K.; Polakova, K.; Tucek, J.; Bourlinos, A.B.; Zboril, R. Toxicity of carbon dots – Effect of surface functionalization on the cell viability, reactive oxygen species generation and cell cycle. *Carbon* **2016**, *99*, 238-248, https://doi.org/10.1016/j.carbon.2015.12.027.
146. Juzenas, P.; Kleinauskas, A.; George Luo, P.; Sun, Y.-P. Photoactivatable carbon nanodots for cancer therapy. *Appl. Phys. Lett.* **2013**, *103*, 063701, https://doi.org/10.1063/1.4817787.
147. Beack, S.; Kong, W.H.; Jung, H.S.; Do, I.H.; Han, S.; Kim, H.; Kim, K.S.; Yun, S.H.; Hahn, S.K. Photodynamic therapy of melanoma skin cancer using carbon dot – chlorin e6 – hyaluronate conjugate. *Acta Biomater.* **2015**, *26*, 295-305, https://doi.org/10.1016/j.actbio.2015.08.027.
148. Sharma, G.; Anabousi, S.; Ehrhardt, C.; Ravi Kumar, M.N.V. Liposomes as targeted drug delivery systems in the treatment of breast cancer. *J. Drug Target.* **2006**, *14*, 301-310, https://doi.org/10.1080/10611860600809112.
149. Kim, K.S.; Hur, W.; Park, S.-J.; Hong, S.W.; Choi, J.E.; Goh, E.J.; Yoon, S.K.; Hahn, S.K. Bioimaging for Targeted Delivery of Hyaluronic Acid Derivatives to the Livers in Cirrhotic Mice Using Quantum Dots. *ACS Nano* **2010**, *4*, 3005-3014, https://doi.org/10.1021/nn100589y.
150. Cao, X.; Deng, W.; Qu, R.; Yu, Q.; Li, J.; Yang, Y.; Cao, Y.; Gao, X.; Xu, X.; Yu, J. Non-Viral Co-Delivery of the Four Yamanaka Factors for Generation of Human Induced Pluripotent Stem Cells via Calcium Phosphate Nanocomposite Particles. *Adv. Funct. Mater.* **2013**, *23*, 5403-5411, https://doi.org/10.1002/adfm.201203646.
151. Lim, S.Y.; Shen, W.; Gao, Z. Carbon quantum dots and their applications. *Chem. Soc. Rev.* **2015**, *44*, 362-381, https://doi.org/10.1039/C4CS00269E.
152. Liu, Z.; Chen, X.; Zhang, X.; Gooding, J.J.; Zhou, Y. Carbon-Quantum-Dots-Loaded Mesoporous Silica Nanocarriers with pH-Switchable Zwitterionic Surface and Enzyme-Responsive Pore-Cap for Targeted Imaging and Drug Delivery to Tumor. *Adv. Healthc. Mater.* **2016**, *5*, 1401-1407, https://doi.org/10.1002/adhm.201600002.
153. Yuan, F.; Yuan, T.; Sui, L.; Wang, Z.; Xi, Z.; Li, Y.; Li, X.; Fan, L.; Tan, Z.a.; Chen, A.; Jin, M.; Yang, S. Engineering triangular carbon quantum dots with unprecedented narrow bandwidth emission for multicolored LEDs. *Nat. Commun.* **2018**, *9*, 2249, https://doi.org/10.1038/s41467-018-04635-5.
154. Yang, X.; Yan, D. Long-afterglow metal–organic frameworks: reversible guest-induced phosphorescence tunability. *Chem. Sci.* **2016**, *7*, 4519-4526, https://doi.org/10.1039/C6SC00563B.
155. Yuan, F.; Wang, Y.-K.; Sharma, G.; Dong, Y.; Zheng, X.; Li, P.; Johnston, A.; Bappi, G.; Fan, J.Z.; Kung, H.; Chen, B.; Saidaminov, M.I.; Singh, K.; Voznyy, O.; Bakr, O.M.; Lu, Z.-H.; Sargent, E.H. Bright high-colour-purity deep-blue carbon dot light-emitting diodes via efficient edge amination. *Nat. Photonics* **2020**, *14*, 171-176, https://doi.org/10.1038/s41566-019-0557-5.
156. Bemidinezhad, A.; Abolhassani, Y.; Feiz, K.; Parsa-kondelaji, M.; Soukhtanloo, M. Carbon and phosphorus quantum dots: Advancing radiotherapy through innovative radiosensitization. *Biochem. Biophys. Res. Commun.* **2025**, *773*, 152054, https://doi.org/10.1016/j.bbrc.2025.152054.
157. Zhu, Z.; Ma, J.; Wang, Z.; Mu, C.; Fan, Z.; Du, L.; Bai, Y.; Fan, L.; Yan, H.; Phillips, D.L.; Yang, S. Efficiency Enhancement of Perovskite Solar Cells through Fast Electron Extraction: The Role of Graphene Quantum Dots. *J. Am. Chem. Soc.* **2014**, *136*, 3760-3763, https://doi.org/10.1021/ja4132246.
158. Wang, Z.; Liu, Y.; Zhen, S.; Li, X.; Zhang, W.; Sun, X.; Xu, B.; Wang, X.; Gao, Z.; Meng, X. Gram-Scale Synthesis of 41% Efficient Single-Component White-Light-Emissive Carbonized Polymer Dots

with Hybrid Fluorescence/Phosphorescence for White Light-Emitting Diodes. *Adv. Sci.* **2020**, *7*, 1902688, https://doi.org/10.1002/advs.201902688.

159. Yang, L.; Jackson, J.C.; Camargos, C.H.M.; Torres Maia, M.; Martinez, D.S.T.; Jardim de Paula, A.; Rezende, C.A.; Faria, A.F. Thin-Film Composite Polyamide Membranes Decorated with Photoactive Carbon Dots for Antimicrobial Applications. *ACS Appl. Nano Mater.* **2024**, *7*, 1477-1490, https://doi.org/10.1021/acsanm.3c05880.
160. Pan, C.; He, J.; Zhu, J.; Li, S.; Li, W.; Yang, W.; Li, W. Corrosion Control by Carbon-Based Nanomaterials: A Review. *ACS Appl. Nano Mater.* **2024**, *7*, 2515-2528, https://doi.org/10.1021/acsanm.3c05547.
161. Mihalache, I.; Radoi, A.; Mihaila, M.; Munteanu, C.; Marin, A.; Danila, M.; Kusko, M.; Kusko, C. Charge and energy transfer interplay in hybrid sensitized solar cells mediated by graphene quantum dots. *Electrochimica Acta* **2015**, *153*, 306-315, https://doi.org/10.1016/j.electacta.2014.11.200.
162. Liu, C.; Chang, K.; Guo, W.; Li, H.; Shen, L.; Chen, W.; Yan, D. Improving charge transport property and energy transfer with carbon quantum dots in inverted polymer solar cells. *Appl. Phys. Lett.* **2014**, *105*, 073306, https://doi.org/10.1063/1.4893994.
163. Wang, B.; Wang, H.; Hu, Y.; Waterhouse, G.I.N.; Lu, S. Carbon Dot Based Multicolor Electroluminescent LEDs with Nearly 100% Exciton Utilization Efficiency. *Nano Lett.* **2023**, *23*, 8794-8800, https://doi.org/10.1021/acs.nanolett.3c02271.
164. Xie, C.; Nie, B.; Zeng, L.; Liang, F.-X.; Wang, M.-Z.; Luo, L.; Feng, M.; Yu, Y.; Wu, C.-Y.; Wu, Y.; Yu, S.-H. Core–Shell Heterojunction of Silicon Nanowire Arrays and Carbon Quantum Dots for Photovoltaic Devices and Self-Driven Photodetectors. *ACS Nano* **2014**, *8*, 4015-4022, https://doi.org/10.1021/nn501001j.
165. Zheng, S.; Mei, X.; Chen, J.; Johansson, E.M.J.; Zhang, X. Colloidal quantum dot for infrared-absorbing solar cells: State-of-the-art and prospects. *Nano Res. Energy* **2024**, *3*, e9120095, https://doi.org/10.26599/NRE.2023.9120095.
166. Liu, W.-W.; Feng, Y.-Q.; Yan, X.-B.; Chen, J.-T.; Xue, Q.-J. Superior Micro-Supercapacitors Based on Graphene Quantum Dots. *Adv. Funct. Mater.* **2013**, *23*, 4111-4122, https://doi.org/10.1002/adfm.201203771.
167. Qu, S.; Liu, X.; Guo, X.; Chu, M.; Zhang, L.; Shen, D. Amplified Spontaneous Green Emission and Lasing Emission From Carbon Nanoparticles. *Adv. Funct. Mater.* **2014**, *24*, 2689-2695, https://doi.org/10.1002/adfm.201303352.
168. Madkhali, O. Sappanwood-derived green luminescent carbon dots for enhancing performance of dye-sensitized solar cell. *J. Mater. Sci.: Mater. Electron.* **2024**, *35*, 1691, https://doi.org/10.1007/s10854-024-13454-y.
169. Zhang, W.F.; Zhu, H.; Yu, S.F.; Yang, H.Y. Observation of Lasing Emission from Carbon Nanodots in Organic Solvents. *Adv. Mater.* **2012**, *24*, 2263-2267, https://doi.org/10.1002/adma.201104950.
170. Vercelli, B. The Role of Carbon Quantum Dots in Organic Photovoltaics: A Short Overview. *Coatings* **2021**, *11*, 232, https://doi.org/10.3390/coatings11020232.
171. Yuan, F.; Xi, Z.; Shi, X.; Li, Y.; Li, X.; Wang, Z.; Fan, L.; Yang, S. Ultrastable and Low-Threshold Random Lasing from Narrow-Bandwidth-Emission Triangular Carbon Quantum Dots. *Adv. Opt. Mater.* **2019**, *7*, 1801202, https://doi.org/10.1002/adom.201801202.
172. Hou, H.; Banks, C.E.; Jing, M.; Zhang, Y.; Ji, X. Carbon Quantum Dots and Their Derivative 3D Porous Carbon Frameworks for Sodium-Ion Batteries with Ultralong Cycle Life. *Adv. Mater.* **2015**, *27*, 7861-7866, https://doi.org/10.1002/adma.201503816.
173. Sarkar, K.; Devi, P.; Lata, A.; Ghosh, R.; Kumar, P. Engineering carbon quantum dots for enhancing the broadband photoresponse in a silicon process-line compatible photodetector. *J. Mater. Chem. C* **2019**, *7*, 13182-13191, https://doi.org/10.1039/C9TC04519H.
174. Hinterberger, V.; Wang, W.; Damm, C.; Wawra, S.; Thoma, M.; Peukert, W. Microwave-assisted one-step synthesis of white light-emitting carbon dot suspensions. *Opt. Mater.* **2018**, *80*, 110-119, https://doi.org/10.1016/j.optmat.2018.04.039.
175. Ogi, T.; Aishima, K.; Permatasari, F.A.; Iskandar, F.; Tanabe, E.; Okuyama, K. Kinetics of nitrogen-doped carbon dot formation via hydrothermal synthesis. *New J. Chem.* **2016**, *40*, 5555-5561, https://doi.org/10.1039/C6NJ00009F.
176. Ali, M.; Riaz, R.; Bae, S.; Lee, H.-S.; Jeong, S.H.; Ko, M.J. Layer-by-Layer Self-Assembly of Hollow Nitrogen-Doped Carbon Quantum Dots on Cationized Textured Crystalline Silicon Solar Cells for an

Efficient Energy Down-Shift. *ACS Appl. Mater. Interfaces* **2020**, *12*, 10369-10381, https://doi.org/10.1021/acsami.9b21087.
177. Lin, H.; Huang, J.; Ding, L. Preparation of Carbon Dots with High-Fluorescence Quantum Yield and Their Application in Dopamine Fluorescence Probe and Cellular Imaging. *J. Nanomater.* **2019**, *2019*, 5037243, https://doi.org/10.1155/2019/5037243.
178. Acharya, B.; Behera, A.; Behera, S.; Moharana, S. Carbon quantum dots: A systematic overview of recent developments in synthesis, properties, and novel therapeutic applications. *Inorg. Chem. Commun.* **2024**, *165*, 112492, https://doi.org/10.1016/j.inoche.2024.112492.

Publisher's Note & Disclaimer